Journal of Engineering Mathematics **47:** 17–43, 2003.

A new formalism for time-dependent electromagnetic scattering from a bounded obstacle

MARIA CRISTINA RECCHIONI[1] and FRANCESCO ZIRILLI[2]
[1]*Istituto di Teoria delle Decisioni e Finanza Innovativa (DE.F.IN.), Università di Ancona, Piazza Martelli 8, 60121 Ancona, Italy e-mail: recchioni@posta.econ.unian.it*
[2]*Dipartimento di Matematica "G. Castelnuovo", Università di Roma "La Sapienza", Piazzale Aldo Moro 2, 00185 Roma, Italy e-mail: f.zirilli@caspur.it*

Received 10 August 2001; accepted in revised form 14 February 2003

Abstract. In this paper a time-dependent three-dimensional electromagnetic scattering problem is considered. Let $\mathbf{R}^3$ be the three-dimensional real Euclidean space filled with a medium of electric permittivity ϵ, magnetic permeability μ and zero electric conductivity. The quantities ϵ, μ are positive constants and there are no free charges in the space and the free current is taken to be zero. Let $\Omega \subset \mathbf{R}^3$ be a bounded simply connected obstacle with a locally Lipschitz boundary $\partial\Omega$, that is assumed to have a nonnegative constant boundary electromagnetic impedance. The limit cases of perfectly conducting and perfectly insulating obstacles are studied. An incoming electromagnetic wave packet that hits Ω is considered, and a method that solves the Maxwell equations to compute the corresponding electromagnetic field scattered by Ω as a superposition of time harmonic electromagnetic waves is proposed. These time-harmonic electromagnetic waves are the solutions of exterior boundary-value problems for the vector Helmholtz equation with the divergence-free condition and they are computed with an 'operator expansion' method that generalizes the method presented by L. Fatone *et al.* [J. Math. Phys. 40 (1999) 4859–4887]. The method proposed here is computationally very efficient. In fact, it is highly parallelizable with respect to time and space variables. Several numerical experiments obtained with a parallel implementation of the method are shown. The numerical results obtained are discussed from a numerical and a physical point of view. The quantitative character of the numerical experiments shown is established. The website: *http://www.econ.unian.it/recchioni/w4/* contains some animations relative to the numerical experiments.

Key words: electromagnetic obstacle scattering, Maxwell's equations, operator expansion method.

1. Introduction

In this paper we consider the following problem:
Problem 1: Given an obstacle $\Omega \subset \mathbf{R}^3$ open, bounded, simply connected, with Lipschitz continuous boundary and its electromagnetic boundary impedance χ, immersed in a homogeneous isotropic medium and given an incoming electromagnetic field propagating in the medium, compute the electromagnetic field generated by the obstacle when hit by the incoming field. In Figure 1 we sketch the situation described above.

The mathematical model used to study *Problem 1* is given by the time-dependent Maxwell equations. In particular, we assume that the electric permittivity $\epsilon > 0$, the magnetic permeability $\mu > 0$ of the medium and the electromagnetic boundary impedance $\chi \geq 0$ are constant. Moreover, we assume that the free current is zero, that no free charges are present and that the electromagnetic incoming field can be represented as a superposition of time-harmonic electromagnetic fields. This last assumption allows us to solve *Problem 1* in the frequency domain and then to come back to the time domain.

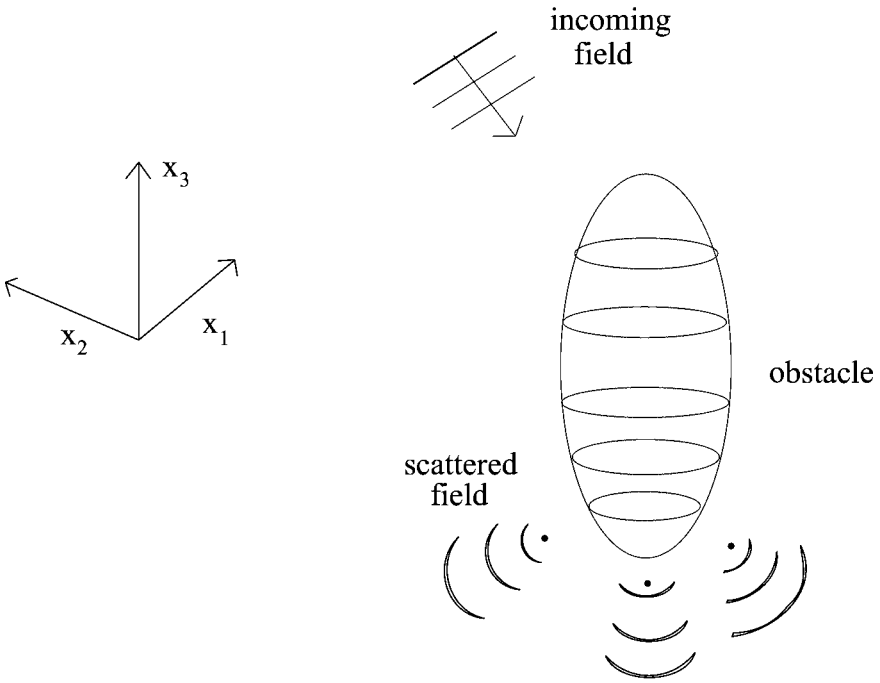

Figure 1. Sketch of the scattering problem considered.

As suggested in [1] and [2], an ideal numerical method to solve time-dependent Maxwell equations should fulfill the following conditions:

($r1$) the electric field must satisfy Gauss's law and the magnetic field must be divergence-free;

($r2$) no linear systems have to be solved at each time step;

($r3$) the method should guarantee high-order accuracy;

($r4$) the method should be easily parallelizable;

($r5$) the method should easily handle domains having complex boundary.

The most commonly used solvers for time-dependent Maxwell equations can be classified as differential-equation-based techniques (finite-difference methods [3], finite-element methods [4]), or time-domain integral-equation-based techniques (finite-volume methods [5], [6], boundary-integral methods [7], [8]).

The finite-difference time-domain methods (see [3] for details) are the most commonly used methods, since they are easy to implement and, sometimes, according to the discretization scheme used, easy to parallelize (conditions ($r2$) and ($r4$)). In fact, an explicit second-order scheme for homogeneous media reproducing the relation 'div curl $= 0$' can be found in Yee [9] and several extensions of this work addressed to verify other vector identities can be found in [10]. Moreover, to satisfy condition ($r1$) several approaches have been used, such as the approach proposed by Munz, Schneider and Sonnerdrüncker [11]. The finite-difference time-domain methods present some difficulties to fulfill condition ($r2$) and ($r5$) (see for example [12] and [13]). However, recently several methods have been developed in order to satisfy the five criteria above. For example Lun and Shen [14] proposed the use of a domain-decomposition technique together with an implicit finite-difference scheme in order to develop an efficient, easily parallelizable numerical method.

A different technique is the finite-element method. This method is well suited for complex-domain geometry, *i.e.*, it naturally fulfills condition $(r5)$. Roughly speaking it is based on a volumetric discretization of the domain under scrutiny and requires local boundary conditions for grid truncation, so that, in general it is not well suited to fulfill condition $(r1)$. Moreover, due to the necessity of using *ad hoc* techniques to verify condition $(r1)$ (see [15], [16]) this method often fails to fulfill condition $(r2)$.

Finally, further solvers for time-dependent Maxwell equations are the time-domain integral-equation-based methods. These methods require only a discretization of the scatterer and they implicitly impose the radiation condition and do not present grid-dispersion errors, that is, they easily fulfill condition $(r1)$ and $(r5)$. The main disadvantage is that they are often considered unstable and computationally expensive with respect to the differential-equation methods. Recently these two lacks have been filled. In fact, stable time-domain integral-equation methods have been reported, for example in [17], and highly performing computational methods of the same type have been reported in [8], [7], [18].

In this paper, we propose a method to solve *Problem 1*. This method could be partially classified as an integral-equation approach. Indeed, it is a new technique that in favourable circumstances specified later can satisfy all five conditions (see Section 7). The method is based on two ideas:

- $(i1)$ to represent the electromagnetic scattered field as a superposition of time-harmonic electromagnetic fields,
- $(i2)$ to compute each time-harmonic electromagnetic field via a suitable generalization of the so-called 'operator-expansion method' proposed in [19].

Idea $(i1)$ is not new; for example, in acoustics it has been used by Heyman in [20], but the use of this idea in the electromagnetic case together with the use of the 'operator expansion' method to compute the time harmonic scattered fields is new and generates an interesting computational method well suited for parallel computation (*i.e.*, condition $(r4)$ is naturally fulfilled). A similar procedure has been used in [21] in the context of acoustic scattering. Roughly speaking, we solve the problem in the frequency domain, and then, via a quadrature formula, we return to the time domain. Under the assumption made above, the solution of the problem in the frequency domain leads to the solution of a set of exterior boundary-value problems for the vector Helmholtz equation with the divergence-free condition, one for each frequency, defined in the exterior of the obstacle Ω, (see (19–22)). These problems are independent from one another and can be solved in parallel. We develop a generalization of the 'operator expansion' method proposed in [19] to solve the exterior boundary-value problems in the frequency domain considered above. We choose the 'operator-expansion method', since it is a highly parallelizable method developed to solve exterior boundary-value problems for the Helmholtz equation. In fact, the 'operator-expansion' method was originally introduced by Milder in [22] to study the time-harmonic acoustic scattering from unbounded surfaces and later developed in [23–31] to deal with several acoustic and electromagnetic scattering problems.

More in detail, the 'operator expansion' method assumes that the solution of the boundary-value problem for the Helmholtz equation defined in the exterior of Ω can be extended to $\mathbf{R}^3 \setminus \Omega_i$ remaining a solution of the Helmholtz equation, where Ω_i is a suitable domain whose closure is contained in Ω. This extension is represented as a single-layer vector potential with a vector density defined on the boundary of Ω_i, *i.e.*, $\partial\Omega_i$. Thanks to this representation formula, the solution of the exterior boundary-value problem outside Ω (see (19–22)) is reduced to the

solution of a linear integral equation for the density defined on $\partial\Omega_i$ (see (38)). This is a linear integral equation of the first kind with a continuous kernel.

This kind of linear integral equations is ill-posed, so that in the specific case considered here we propose to solve it perturbatively. The use of this perturbation series is an attempt to 'cure' the ill-posedness of the integral equation. As an alternative to this perturbation series, the ill-posedness of the integral equation can be approached using standard regularization techniques such as the Tichonov regularization technique. However, in our experience the use of the perturbation series eventually, together with the use of regularization techniques on the integral equations coming up at each order in perturbation theory, gives substantially better results than the use of regularization techniques on the original integral equation.

In particular, we use a series expansion of the unknown vector density, of the integral operator and of the data. The possibility of using these series expansions is based on the availability of a coordinate system (η_1, η_2, η_3) in $\mathbf{R}^3$ such that the boundary of Ω can be represented as a Lipschitz continuous function of two coordinate variables, that is, for example, $\eta_3 = g(\eta_1, \eta_2)$ where (η_1, η_2) belongs to a suitable domain of definition and g is a given function. The expansions are built along the η_3 coordinate axis and have as base point a second surface $\partial\Omega_r$, boundary of Ω_r, where Ω_r is a bounded domain that contains the closure of Ω_i. Note that in this paper we choose as (η_1, η_2, η_3) coordinate system the spherical coordinates in $\mathbf{R}^3$ with pole in the origin; more general choices are considered in [28]. Via these series expansions, the solution of the integral equation corresponding to imposing the boundary condition satisfied by the scattered field on $\partial\Omega$ using an unknown density defined on $\partial\Omega_i$ is transformed in a sequence of integral equations, one for each order in perturbation theory. These integral equations correspond to imposing the appropriate condition derived from perturbation theory on $\partial\Omega_r$ using unknown densities defined on $\partial\Omega_i$. Choosing the 'distance' between $\partial\Omega$ and $\partial\Omega_r$ sufficiently 'small', we can satisfy accurately condition $(r3)$ with a few terms of the series expansion and we can deal with rather general obstacles. In this paper, for simplicity, we choose the base point $\partial\Omega_r$ and $\partial\Omega_i$ to be the surface of two spheres and we choose the vector spherical harmonics as basis to represent the datum, the unknown and the integral operators. These choices allow us to solve a diagonal linear system at each order in perturbation theory and to develop a numerical method that naturally fulfills conditions $(r1)$, $(r2)$ and $(r4)$ also when non-trivial obstacles are considered (see the corrugated surface, *i.e.*, Obstacle 5, proposed in Section 6). However, these choices affect the accuracy of the method (*i.e.*, condition $(r3)$). In fact, the perturbation solution is based on the assumption that the boundary of the obstacle is a perturbation of the 'base point' of the series expansion, $\partial\Omega_r$, so that the perturbation solution is accurate when the 'distance' of the boundary of the obstacle from the boundary of the sphere Ω_r is 'small' (see Tables 1–5). However, we note that rather difficult obstacles for many others time-domain Maxwell solvers can be treated satisfactorily with the method proposed here when we choose (η_1, η_2, η_3) to be the spherical coordinate system and when Ω_i, Ω_r are chosen to be spheres, that is, $\Omega_i = B_a$ and $\Omega_r = B_1$, where for $R > 0$ $B_R = \{ \underline{x} \in \mathbf{R}^3 \, | \|\underline{x}\| < R\}$ is the sphere of radius R and center the origin (see for example Obstacle 5 (Table 4)). Later we use B and ∂B instead of B_1 and ∂B_1, respectively. Finally, we note that this simple choice has the advantage of avoiding the use of regularization methods in the solution of the integral equations on the sphere. In fact, when the basis of the vector spherical harmonic functions is used, the solution of these integral equations is reduced to the solution of diagonal linear systems that are independent of the sphere B_a and depend only on $\partial\Omega$ and B_1. This is an interesting feature of the implementation of the 'operator

Table 1. $\chi = 0$, $\max_{\underline{\hat{x}} \in \partial B} |\xi(\underline{\hat{x}}) - 1| = 0$

$\frac{\omega}{c}$	$\epsilon^{16}_{1,\underline{F}_{\omega,\underline{\gamma}}}$	$\epsilon^{16}_{2,\underline{F}_{\omega,\underline{\gamma}}}$	$\epsilon^{16}_{3,\underline{F}_{\omega,\underline{\gamma}}}$
1	$2{\cdot}19 \times 10^{-7}$	$3{\cdot}59 \times 10^{-7}$	$5{\cdot}00 \times 10^{-7}$
2	$5{\cdot}51 \times 10^{-7}$	$1{\cdot}27 \times 10^{-7}$	$4{\cdot}61 \times 10^{-7}$
4	$5{\cdot}79 \times 10^{-7}$	$7{\cdot}56 \times 10^{-7}$	$6{\cdot}69 \times 10^{-7}$
8	$3{\cdot}80 \times 10^{-7}$	$5{\cdot}20 \times 10^{-7}$	$5{\cdot}43 \times 10^{-7}$

expansion' method proposed in this paper, since in practice the explicit choice of the sphere B_a is not really necessary.

We have noted that the 'operator expansion' method should be classified as an integral-equation approach. We conclude this outline of the 'operator expansion' method discussing some features of the other integral-equation methods that make them different from the approach proposed here. In particular, we note that the integral equations coming from the boundary-integral methods are usually of the second kind, that is, they are well-posed integral equations but have singular kernels, and, when the boundary of the obstacle is only Lipschitz continuous, involve singular integral operators (see [32], [33]). The numerical treatment of these singular integral operators is a challenging problem. Moreover, depending on the shape of the boundary, the discretization process on this boundary may not be 'easy' and the resulting algorithms may not be well suited for parallel computation. That is, conditions $(r2)$, $(r4)$ and $(r5)$ cannot be satisfied simultaneously. In fact, the linear systems coming from the discretization of the integral equation obtained from the boundary-integral method is usually a dense linear system (*i.e.*, it is not sparse or diagonal).

The paper is organized as follows. In Section 2 we describe the mathematical model. In Section 3 we describe the basic ideas of the method proposed and the underlying assumptions. In Section 4 we give the expansion of the time-harmonic electromagnetic fields, in Section 5 we describe the computational method and in Section 6 some numerical results obtained with a parallel implementation of the method presented in Section 3, 4 and 5 are presented. In particular, we consider obstacles whose boundary is only a locally Lipschitz surface (cutted octahedron (Figure 2 (3)), holed sphere (Figure 2 (4))) so that some interesting physical phenomena due to the faces, edges, vertices and cavities present in the obstacles can be shown. We show that the computational cost of the algorithm proposed in this paper is $O(S^2 L^2_{\max} N_1 N_2 N_3 M)$, when $S \to +\infty$, $L_{\max} \to +\infty$, N_1, N_2, $N_3 \to +\infty$, $M \to \infty$, where $N_1 \cdot N_2 \cdot N_3$ is the number of quadrature points used in the integral-representation formulae for the scattered electromagnetic field $\underline{\mathcal{E}}^s$, $\underline{\mathcal{B}}^s$, S is the order at which the perturbation expansion is truncated, $2(L_{\max}+2)L_{\max}$ is the number of vector spherical harmonics used to represent the unknown densities, that is the series in vector spherical harmonics are truncated for $l = L_{\max}$, and M is the number of quadrature points used to approximate the double integrals on ∂B (see formula (68)). The unknown densities are assumed to be tangential to ∂B. For this reason we use only $2(L_{\max}+2)L_{\max}$ vector spherical harmonics to represent the densities. We note that we obtain satisfactory results using always $L_{\max} \leq 20$ and $S \leq 10$. Moreover in many applications of practical interest we can choose $N_2 = N_3 = 1$ (see Section 6) reducing the burden of the previous formula and at each order in perturbation theory we can compute in parallel the integrals reducing the computational cost to $O(S^2 L^2_{\max} N_1 N_2 N_3 M/N_p)$, where

Table 2. Comparison between the analytical solution and the numerical solution: Table of $e^S_{L_{\max},R}$ as a function of R and S when $\chi = 0$, $\Omega = B_R$

$R \setminus S$	0	1	2	3	4	5	6	7	8	9
1·05	$9{\cdot}67 \times 10^{-2}$	$3{\cdot}87 \times 10^{-3}$	$5{\cdot}37 \times 10^{-4}$	$4{\cdot}73 \times 10^{-5}$	$4{\cdot}41 \times 10^{-5}$	$3{\cdot}75 \times 10^{-7}$	$7{\cdot}51 \times 10^{-13}$	$3{\cdot}76 \times 10^{-17}$	$3{\cdot}76 \times 10^{-17}$	$3{\cdot}76 \times 10^{-17}$
1·1	$1{\cdot}74 \times 10^{-1}$	$1{\cdot}39 \times 10^{-2}$	$3{\cdot}80 \times 10^{-3}$	$6{\cdot}71 \times 10^{-4}$	$1{\cdot}32 \times 10^{-4}$	$2{\cdot}54 \times 10^{-5}$	$4{\cdot}99 \times 10^{-6}$	$9{\cdot}86 \times 10^{-7}$	$7{\cdot}05 \times 10^{-8}$	$8{\cdot}75 \times 10^{-17}$
1·2	$2{\cdot}87 \times 10^{-1}$	$4{\cdot}65 \times 10^{-2}$	$2{\cdot}41 \times 10^{-2}$	$8{\cdot}48 \times 10^{-3}$	$3{\cdot}33 \times 10^{-3}$	$1{\cdot}28 \times 10^{-3}$	$4{\cdot}96 \times 10^{-4}$	$1{\cdot}92 \times 10^{-4}$	$7{\cdot}39 \times 10^{-5}$	$2{\cdot}86 \times 10^{-5}$
1·4	$4{\cdot}30 \times 10^{-1}$	$1{\cdot}44 \times 10^{-1}$	$1{\cdot}25 \times 10^{-1}$	$8{\cdot}69 \times 10^{-2}$	$6{\cdot}81 \times 10^{-2}$	$5{\cdot}25 \times 10^{-2}$	$4{\cdot}06 \times 10^{-2}$	$3{\cdot}14 \times 10^{-2}$	$2{\cdot}42 \times 10^{-2}$	$1{\cdot}87 \times 10^{-2}$
1·8	$6{\cdot}53 \times 10^{-1}$	$4{\cdot}17 \times 10^{-1}$	$4{\cdot}22 \times 10^{-1}$	$5{\cdot}71 \times 10^{-1}$	$8{\cdot}83 \times 10^{-1}$	$1{\cdot}36 \times 10^{0}$	$2{\cdot}10 \times 10^{0}$	$3{\cdot}25 \times 10^{0}$	$5{\cdot}02 \times 10^{0}$	$7{\cdot}75 \times 10^{0}$

Table 3. Cut octahedron: $\chi = \infty$, $\max_{\underline{\hat{x}} \in \partial B} |\xi(\underline{\hat{x}}) - 1| = 0{\cdot}4$

$\frac{\omega}{c}$	e^1_{16}	e^2_{16}	e^3_{16}	e^4_{16}	e^5_{16}	e^6_{16}	e^7_{16}	e^8_{16}	e^9_{16}
0·5	$9{\cdot}30 \times 10^{-2}$	$6{\cdot}66 \times 10^{-2}$	$3{\cdot}79 \times 10^{-2}$	$2{\cdot}09 \times 10^{-2}$	$1{\cdot}48 \times 10^{-2}$	$6{\cdot}27 \times 10^{-3}$	$4{\cdot}67 \times 10^{-3}$	$4{\cdot}61 \times 10^{-3}$	$1{\cdot}23 \times 10^{-3}$
1	$6{\cdot}55 \times 10^{-2}$	$4{\cdot}80 \times 10^{-2}$	$2{\cdot}65 \times 10^{-2}$	$1{\cdot}55 \times 10^{-2}$	$1{\cdot}55 \times 10^{-2}$	$5{\cdot}03 \times 10^{-3}$	$5{\cdot}48 \times 10^{-3}$	$4{\cdot}20 \times 10^{-3}$	$1{\cdot}94 \times 10^{-3}$
2	$1{\cdot}47 \times 10^{-1}$	$4{\cdot}55 \times 10^{-2}$	$3{\cdot}28 \times 10^{-2}$	$1{\cdot}86 \times 10^{-2}$	$1{\cdot}63 \times 10^{-2}$	$5{\cdot}28 \times 10^{-3}$	$5{\cdot}65 \times 10^{-3}$	$3{\cdot}58 \times 10^{-3}$	$2{\cdot}29 \times 10^{-3}$
4	$2{\cdot}96 \times 10^{-1}$	$6{\cdot}48 \times 10^{-2}$	$3{\cdot}78 \times 10^{-2}$	$2{\cdot}77 \times 10^{-2}$	$2{\cdot}07 \times 10^{-2}$	$1{\cdot}22 \times 10^{-2}$	$7{\cdot}94 \times 10^{-3}$	$5{\cdot}83 \times 10^{-3}$	$2{\cdot}85 \times 10^{-3}$
8	$5{\cdot}54 \times 10^{-1}$	$3{\cdot}14 \times 10^{-1}$	$1{\cdot}68 \times 10^{-1}$	$5{\cdot}96 \times 10^{-2}$	$3{\cdot}66 \times 10^{-2}$	$2{\cdot}27 \times 10^{-2}$	$1{\cdot}32 \times 10^{-2}$	$1{\cdot}21 \times 10^{-2}$	$7{\cdot}19 \times 10^{-3}$

Table 4. Obstacle 5: $\chi = 0$, $\max_{\hat{\underline{x}} \in \partial B} |\xi(\hat{\underline{x}}) - 1| = 0{\cdot}2$

$\frac{\omega}{c}$	e_{16}^1	e_{16}^2	e_{16}^3	e_{16}^4	e_{16}^5	e_{16}^6	e_{16}^7	e_{16}^8	e_{16}^9
0·5	$2{\cdot}29 \times 10^{-1}$	$2{\cdot}4 \times 10^{-2}$	$1{\cdot}45 \times 10^{-3}$	$1{\cdot}21 \times 10^{-4}$	$1{\cdot}01 \times 10^{-5}$	$7{\cdot}83 \times 10^{-6}$	$7{\cdot}85 \times 10^{-8}$	$1{\cdot}96 \times 10^{-9}$	$7{\cdot}50 \times 10^{-12}$
1	$1{\cdot}78 \times 10^{-1}$	$1{\cdot}46 \times 10^{-2}$	$4{\cdot}04 \times 10^{-3}$	$7{\cdot}18 \times 10^{-4}$	$1{\cdot}43 \times 10^{-4}$	$2{\cdot}80 \times 10^{-5}$	$5{\cdot}70 \times 10^{-6}$	$1{\cdot}09 \times 10^{-6}$	$9{\cdot}66 \times 10^{-8}$
2	$1{\cdot}83 \times 10^{-1}$	$2{\cdot}60 \times 10^{-2}$	$6{\cdot}16 \times 10^{-3}$	$1{\cdot}53 \times 10^{-3}$	$4{\cdot}40 \times 10^{-4}$	$1{\cdot}25 \times 10^{-4}$	$3{\cdot}55 \times 10^{-5}$	$1{\cdot}01 \times 10^{-5}$	$2{\cdot}90 \times 10^{-6}$
4	$2{\cdot}91 \times 10^{-1}$	$6{\cdot}66 \times 10^{-2}$	$1{\cdot}48 \times 10^{-2}$	$4{\cdot}76 \times 10^{-3}$	$1{\cdot}94 \times 10^{-3}$	$8{\cdot}14 \times 10^{-4}$	$3{\cdot}44 \times 10^{-4}$	$1{\cdot}46 \times 10^{-4}$	$6{\cdot}20 \times 10^{-5}$
8	$5{\cdot}05 \times 10^{-1}$	$2{\cdot}15 \times 10^{-1}$	$6{\cdot}68 \times 10^{-2}$	$2{\cdot}15 \times 10^{-2}$	$1{\cdot}06 \times 10^{-2}$	$6{\cdot}43 \times 10^{-3}$	$4{\cdot}05 \times 10^{-3}$	$2{\cdot}58 \times 10^{-3}$	$1{\cdot}65 \times 10^{-3}$

Table 5. Corrugated Sphere: $\chi = 2$, $\omega/c = 10$, $\max_{\hat{\underline{x}} \in \partial B} |\xi(\hat{\underline{x}}) - 1| = h$

h	e_{16}^1	e_{16}^2	e_{16}^3	e_{16}^4	e_{16}^5	e_{16}^6	e_{16}^7	e_{16}^8	e_{16}^9
0·01	$3{\cdot}42 \times 10^{-2}$	$1{\cdot}13 \times 10^{-3}$	$3{\cdot}02 \times 10^{-5}$	$8{\cdot}24 \times 10^{-7}$	$2{\cdot}13 \times 10^{-8}$	$2{\cdot}14 \times 10^{-11}$	$2{\cdot}12 \times 10^{-21}$	$4{\cdot}72 \times 10^{-26}$	$1{\cdot}10 \times 10^{-34}$
0·1	$3{\cdot}13 \times 10^{-1}$	$1{\cdot}07 \times 10^{-1}$	$2{\cdot}89 \times 10^{-2}$	$7{\cdot}10 \times 10^{-3}$	$1{\cdot}36 \times 10^{-3}$	$2{\cdot}54 \times 10^{-4}$	$3{\cdot}55 \times 10^{-5}$	$8{\cdot}04 \times 10^{-6}$	$1{\cdot}14 \times 10^{-6}$
0·2	$5{\cdot}27 \times 10^{-1}$	$3{\cdot}75 \times 10^{-1}$	$2{\cdot}30 \times 10^{-1}$	$1{\cdot}09 \times 10^{-1}$	$4{\cdot}20 \times 10^{-2}$	$1{\cdot}56 \times 10^{-2}$	$4{\cdot}78 \times 10^{-3}$	$2{\cdot}12 \times 10^{-3}$	$6{\cdot}59 \times 10^{-4}$
0·5	$7{\cdot}92 \times 10^{-1}$	$8{\cdot}16 \times 10^{-1}$	$9{\cdot}88 \times 10^{-1}$	$1{\cdot}29 \times 10^{0}$	$1{\cdot}54 \times 10^{0}$	$1{\cdot}44 \times 10^{0}$	$1{\cdot}33 \times 10^{0}$	$1{\cdot}54 \times 10^{0}$	$1{\cdot}10 \times 10^{0}$

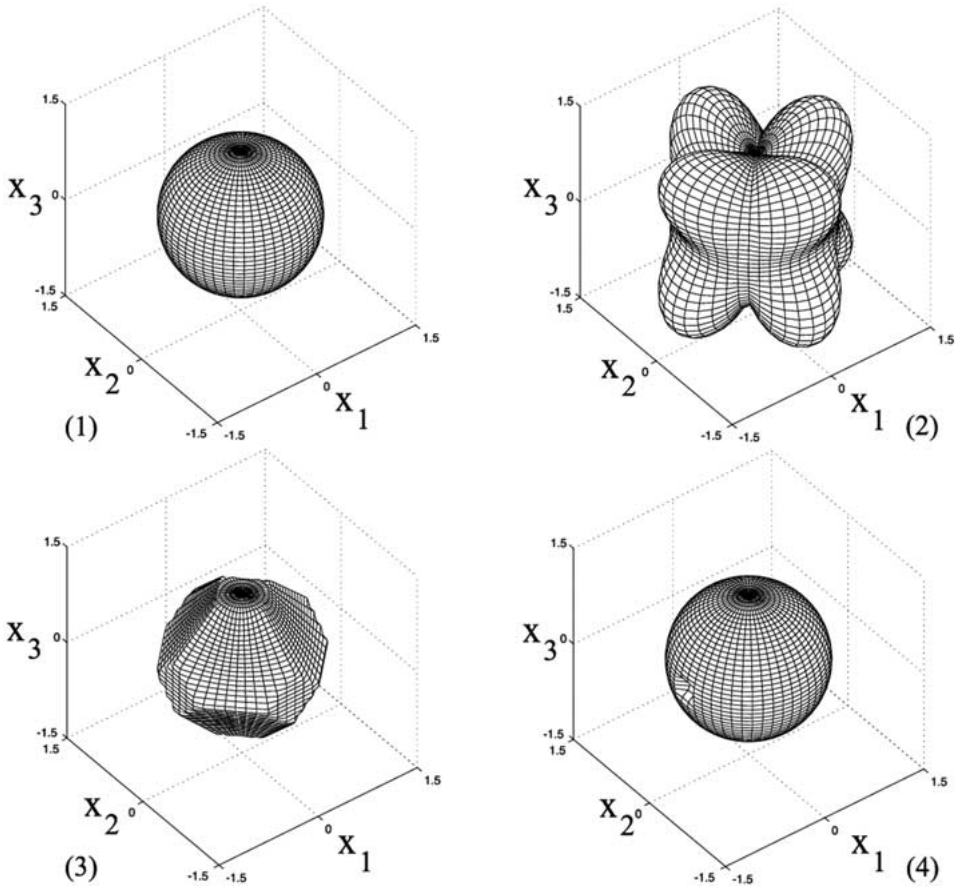

Figure 2. Obstacles: Sphere (1), Corrugated Sphere ($h = 0.7$) (2), Cutted Octahedron (3), Holed Sphere (4).

N_p is the number of processors used. Note that this computational cost is relative to the particular implementation of the operator-expansion method proposed in this paper, that is to the choice of the spherical coordinate system, the choice $\Omega_i = B_a$ and $\Omega_r = B_1, 0 < a < 1$ and the use of the vector spherical harmonics as basis to represent the datum, the unknown and the integral operators.

It is not easy to make comparisons between the computational cost of the proposed algorithm and the computational cost of well-known efficient algorithms such as for example the algorithms proposed in [18] and [8]. Roughly speaking, the number N_s of spatial samples quoted in [8] (that is the number of elements used to decompose the obstacle surface) of a fast multipole method corresponds to the number $2(L_{\max} + 2)L_{\max}$ of vector spherical harmonics and the number N_t of time steps in the time domain (see [8]) corresponds to the number $N_1 \cdot N_2 \cdot N_3$ of time-harmonic fields used in the frequency domain. Hence we can conclude that with these identifications the computational cost of the algorithm proposed here is linear in the number of time steps and in the number of spatial samples when these quantities go to infinity. That is, our method compares favorably with the methods proposed in [8] and [18]. Moreover, the basic ideas of the fast multipole method can be used in the operator-expansion method to generate what should be called 'fast operator-expansion method'. This possibility will be studied in a forthcoming paper.

Moreover, we show some interesting speed-up factors (see Table 6) obtained when running our method on a multiprocessor machine. The numerical results are discussed both from the numerical and the physical point of view. The quantitative character of the numerical results shown is established. Some animations relative to the numerical experience described above can be found in the website: *http://www.econ.unian.it/recchioni/w4/*. In Section 7 we present some final remarks and we suggest some ideas for further investigation.

2. The mathematical model

Let us begin by introducing some notations. Let $\mathbf{R}$ be the set of real numbers, N be a positive integer and $\mathbf{R}^N$ be the N dimensional real Euclidean space. Let $\underline{x} = (x_1, x_2, x_3)^T \in \mathbf{R}^3$ be a generic vector, where the superscript T denotes the transposition operation. In $\mathbf{R}^3$ we denote with $(\cdot, \cdot)$ the Euclidean scalar product, with $\|\cdot\|$ the corresponding Euclidean vector norm and with $[\cdot, \cdot]$ the vector product. Sometimes we use $(\cdot, \cdot)$ and $[\cdot, \cdot]$ with complex vectors as arguments to denote the real Euclidean scalar and vector product of complex vectors respectively. Let $\mathbf{C}$ be the set of complex numbers, i be the imaginary unit, when $z \in \mathbf{C}$ we denote with $\overline{z}$ the complex conjugate of z, with $|z|$ the modulus of z and with $\mathfrak{R}frake(z)$, $\mathfrak{Im}(z)$ the real and imaginary part of z respectively. Let $a > 0$ be a constant, $B_a = \{\underline{x} \in \mathbf{R}^3 | \, \|\underline{x}\| < a\}$ and let ∂B_a be its boundary. Let $\Omega \subset \mathbf{R}^3$ be a bounded simply connected open domain with locally Lipschitz boundary $\partial\Omega$ and let $\overline{\Omega}$ be the closure of Ω. We observe that the domains with locally Lipschitz boundary include polyhedra. The domain Ω is the obstacle that scatters the incoming electromagnetic field. We assume that Ω contains the origin so that there exists $a > 0$ such that $\overline{B_a} \subset \Omega$. We denote with $\chi \in \mathbf{R}$, $\chi \geq 0$, the electromagnetic boundary impedance of $\partial\Omega$ and we assume that χ is a constant. When $\partial\Omega$ is a locally Lipschitz boundary, the outward unit normal vector to $\partial\Omega$, $\underline{n}(\underline{x}) = (n_1(\underline{x}), n_2(\underline{x}), n_3(\underline{x}))^T \in \mathbf{R}^3$, $\underline{x} \in \partial\Omega$ exists almost everywhere on the boundary $\partial\Omega$ (see [34, Lemma 2.42, p. 88]). We consider $\mathbf{R}^3$ filled with a homogeneous isotropic medium characterized by electric permittivity $\epsilon > 0$, magnetic permeability $\mu > 0$ and zero electric conductivity. We assume ϵ, μ to be constants and the free-charge density and the free current to be zero. When the obstacle Ω is present and the incoming electromagnetic field (*i.e.*, the electric field $\underline{\mathcal{E}}^i(\underline{x}, t)$ and the magnetic induction vector field $\underline{\mathcal{B}}^i(\underline{x}, t)$, $(\underline{x}, t) \in \mathbf{R}^3 \times \mathbf{R}$) hits the obstacle Ω, a scattered electromagnetic field is generated and we denote with $\underline{\mathcal{E}}^s(\underline{x}, t)$, $\underline{\mathcal{B}}^s(\underline{x}, t)$, $(\underline{x}, t) \in (\mathbb{R}^3 \backslash \overline{\Omega}) \times \mathbf{R}$ the scattered electric field and the scattered magnetic vector induction field, respectively. We use the M.K.S. unit system (see [35, p. 16]) to write the necessary equations. We assume that the incoming electromagnetic field $\underline{\mathcal{E}}^i(\underline{x}, t)$, $\underline{\mathcal{B}}^i(\underline{x}, t)$, $(\underline{x}, t) \in \mathbf{R}^3 \times \mathbf{R}$ satisfies the Maxwell equations, that is, Equations (1–4) in $\mathbf{R}^3 \times \mathbf{R}$. In these hypotheses the electromagnetic field $\underline{\mathcal{E}}^s(\underline{x}, t)$, $\underline{\mathcal{B}}^s(\underline{x}, t)$, $(\underline{x}, t) \in (\mathbb{R}^3 \backslash \overline{\Omega}) \times \mathbf{R}$ satisfies the following equations:

$$\left(\mathrm{curl}\underline{\mathcal{E}}^s + \frac{\partial \underline{\mathcal{B}}^s}{\partial t}\right)(\underline{x}, t) = \underline{0}, \, (\underline{x}, t) \in (\mathbf{R}^3 \backslash \overline{\Omega}) \times \mathbf{R}, \tag{1}$$

$$\left(\mathrm{curl}\underline{\mathcal{B}}^s - \frac{1}{c^2}\frac{\partial \underline{\mathcal{E}}^s}{\partial t}\right)(\underline{x}, t) = \underline{0}, \, (\underline{x}, t) \in (\mathbf{R}^3 \backslash \overline{\Omega}) \times \mathbf{R}, \tag{2}$$

$$\mathrm{div}\, \underline{\mathcal{B}}^s(\underline{x}, t) = 0, \quad (\underline{x}, t) \in (\mathbf{R}^3 \backslash \overline{\Omega}) \times \mathbf{R}, \tag{3}$$

$$\mathrm{div}\, \underline{\mathcal{E}}^s(\underline{x}, t) = 0, \quad (\underline{x}, t) \in (\mathbf{R}^3 \backslash \overline{\Omega}) \times \mathbf{R}, \tag{4}$$

with boundary condition (see [36, p. 1599]):

$$[\underline{n}(\underline{x}), \underline{\mathcal{E}}^s(\underline{x}, t)] - c\chi[\underline{n}(\underline{x}), [\underline{n}(\underline{x}), \underline{\mathcal{B}}^s(\underline{x}, t)]] = \underline{b}(\underline{x}, t),\ (\underline{x}, t) \in \partial\Omega \times \mathbf{R}, \tag{5}$$

where:

$$\underline{b}(\underline{x}, t) = -[\underline{n}(\underline{x}), \underline{\mathcal{E}}^i(\underline{x}, t)] + c\chi[\underline{n}(\underline{x}), [\underline{n}(\underline{x}), \underline{\mathcal{B}}^i(\underline{x}, t)]],\ (\underline{x}, t) \in \partial\Omega \times \mathbf{R}, \tag{6}$$

the following boundary condition at infinity:

$$\underline{\mathcal{E}}^s(\underline{x}, t) = O\left(\frac{1}{r}\right), r \to +\infty, t \in \mathbf{R}, \tag{7}$$

and the radiation condition:

$$[\underline{\mathcal{B}}^s(\underline{x}, t), \underline{\hat{c}}] - \frac{1}{c}\underline{\mathcal{E}}^s(\underline{x}, t) = o\left(\frac{1}{r}\right),\ r \to +\infty,\ t \in \mathbf{R}, \tag{8}$$

where $\underline{0} = (0, 0, 0)^T$, $c = 1/\sqrt{\epsilon\,\mu}$, curl, div and $\partial/\partial t$ denote, respectively, the curl, the divergence operator with respect to the $\underline{x}$ variables and the time derivative, $\underline{\hat{c}} = \underline{x}/\|\underline{x}\|$, $\underline{x} \neq \underline{0}$, $r = \|\underline{x}\|$, and $o(\cdot)$, $O(\cdot)$ are the Landau symbols. We note that the limit cases $\chi = 0$, that is a perfectly conducting obstacle, and $\chi = \infty$, that is a perfectly insulating obstacle, can be treated by adapting the boundary condition (5). In particular, when $\chi = \infty$, the perfectly insulating boundary condition is obtained by dividing (5) by χ and using the fact that $1/\chi = 0$ when $\chi = \infty$. Condition (7) (see [35, p. 485]) says that when the sources of the scattered electromagnetic field are located within a finite distance from the origin, that is on $\partial\Omega$, the intensity of $\underline{\mathcal{E}}^s$ must vanish when $r \to +\infty$. The radiation condition (8) says that the leading order of the scattered electromagnetic field $\underline{\mathcal{E}}^s$, $\underline{\mathcal{B}}^s$ (see [35, p. 26]) is made of divergent spherical waves as $r \to +\infty$. Moreover, condition (7) and (8) implies that $\underline{\mathcal{B}}^s(\underline{x}, t) = O\left(\frac{1}{r}\right)$, $r \to +\infty$, $t \in \mathbf{R}$. Since the incoming electromagnetic field satisfies the Maxwell equations (1–4) in $\mathbf{R}^3 \times \mathbf{R}$, we have that the incoming electric field and the magnetic vector induction field $\underline{\mathcal{E}}^i$, $\underline{\mathcal{B}}^i$ satisfy the vector wave equation in $\mathbf{R}^3 \times \mathbf{R}$, and similarly $\underline{\mathcal{E}}^s$, $\underline{\mathcal{B}}^s$ satisfy the vector wave equation in $(\mathbf{R}^3 \backslash \overline{\Omega}) \times \mathbf{R}$, that is, we have:

$$\underline{\mathcal{E}}^i(\underline{x}, t) = \frac{1}{(2\pi)^4}\int_{\mathbf{R}} \mathrm{d}\omega\, w(\omega) \exp(-\mathrm{i}\omega t) \int_{\partial B} \mathrm{d}s(\underline{\alpha})\underline{V}(\omega, \underline{\alpha}) \exp(\frac{\mathrm{i}\omega}{c}(\underline{x}, \underline{\alpha})),\ (\underline{x}, t) \in \mathbf{R}^3 \times \mathbf{R}, \tag{9}$$

$$\underline{\mathcal{B}}^i(\underline{x}, t) = \frac{1}{(2\pi)^4}\int_{\mathbf{R}} \mathrm{d}\omega\, w(\omega) \exp(-\mathrm{i}\omega t) \int_{\partial B} \mathrm{d}s(\underline{\alpha})\underline{U}(\omega, \underline{\alpha}) \exp(\frac{\mathrm{i}\omega}{c}(\underline{x}, \underline{\alpha})),\ (\underline{x}, t) \in \mathbf{R}^3 \times \mathbf{R}, \tag{10}$$

where $\mathrm{d}s(\underline{\alpha})$ is the surface measure on ∂B, $w(\omega)$ is a suitable positive real-valued function that plays the role of a weight function and $\underline{V}(\omega, \underline{\alpha})$, $\underline{U}(\omega, \underline{\alpha})$ are suitable vector-valued distributions. From Maxwell equations we have:

$$(\underline{V}(\omega, \underline{\alpha}), \underline{\alpha}) = 0, \quad (\underline{U}(\omega, \underline{\alpha}), \underline{\alpha}) = 0,\ \underline{U}(\omega, \underline{\alpha}) = \frac{1}{c}[\underline{\alpha}, \underline{V}(\omega, \underline{\alpha})],\ \underline{\alpha} \in \partial B, \omega \in \mathbf{R}. \tag{11}$$

Note that the function $w(\omega)$ is redundant and is used here only to simplify the notation in the following sections. When $\underline{V}(\omega, \underline{\alpha})$ has support in $\{\,(\omega, \underline{\alpha}) \in \mathbf{R} \times \partial B \mid \underline{\alpha} = \underline{\gamma},\ \underline{\gamma} \in \partial B\,\}$, the integrals in (9), (10) reduce to one-dimensional integrals. We assume that the scattered electromagnetic field can be represented with formulae similar to (9), (10), that is:

$$\underline{\mathcal{E}}^s(\underline{x},t)=\frac{1}{(2\pi)^4}\int_{\mathbf{R}}\mathrm{d}\omega\, w(\omega)\exp(-\mathrm{i}\omega t)\int_{\partial B}\mathrm{d}s(\underline{\alpha})\underline{E}^s_{\omega,\underline{\alpha}}(\underline{x}),\ (\underline{x},t)\in(\mathbf{R}^3\backslash\overline{\Omega})\times\mathbf{R}\,, \tag{12}$$

$$\underline{\mathcal{B}}^s(\underline{x},t)=\frac{1}{(2\pi)^4}\int_{\mathbf{R}}\mathrm{d}\omega\, w(\omega)\exp(-\mathrm{i}\omega t)\int_{\partial B}\mathrm{d}s(\underline{\alpha})\underline{B}^s_{\omega,\underline{\alpha}}(\underline{x}),\ (\underline{x},t)\in(\mathbf{R}^3\backslash\overline{\Omega})\times\mathbf{R}\,. \tag{13}$$

Note that, when the support of $\underline{V}(\omega,\underline{\alpha})$ satisfies the conditions specified previously, also the integrals in (12), (13) reduce to one-dimensional integrals. Since $\underline{\mathcal{E}}^s$, $\underline{\mathcal{B}}^s$ are solutions of problem (1–5), (7), (8), we have that for $\omega\in\mathbf{R}$, $\underline{\alpha}\in\partial B$, the functions $\underline{E}^s_{\omega,\underline{\alpha}}$, $\underline{B}^s_{\omega,\underline{\alpha}}$ are solutions of the following exterior boundary-value problem:

$$\mathrm{curl}\underline{E}^s_{\omega,\underline{\alpha}}(\underline{x})-\mathrm{i}\omega\underline{B}^s_{\omega,\underline{\alpha}}(\underline{x})=\underline{0}\,,\quad \underline{x}\in\mathbf{R}^3\backslash\overline{\Omega}\,, \tag{14}$$

$$\mathrm{curl}\underline{B}^s_{\omega,\underline{\alpha}}(\underline{x})+\frac{\mathrm{i}\omega}{c^2}\underline{E}^s_{\omega,\underline{\alpha}}(\underline{x})=\underline{0}\,,\quad \underline{x}\in\mathbf{R}^3\backslash\overline{\Omega}\,, \tag{15}$$

with the boundary condition:

$$[\underline{n},\underline{E}^s_{\omega,\underline{\alpha}}](\underline{x})-c\chi[\underline{n},[\underline{n},\underline{B}^s_{\omega,\underline{\alpha}}]](\underline{x})=[\underline{n},\underline{b}^s_{\omega,\underline{\alpha}}](\underline{x}),\ \underline{x}\in\partial\Omega, \tag{16}$$

where:

$$\underline{b}^s_{\omega,\underline{\alpha}}(\underline{x})=\exp(\frac{\mathrm{i}\omega}{c}(\underline{x},\underline{\alpha}))\left\{-\underline{V}(\omega,\underline{\alpha})+\chi[\underline{n}(\underline{x}),[\underline{\alpha},\underline{V}(\omega,\underline{\alpha})]]\right\},\ \underline{x}\in\partial\Omega, \tag{17}$$

and the radiation condition at infinity:

$$[\underline{B}^s_{\omega,\underline{\alpha}},\hat{\underline{c}}]-\frac{1}{c}\underline{E}^s_{\omega,\underline{\alpha}}=o(\frac{1}{r}),\ r\to+\infty\,. \tag{18}$$

We note that the constants in formulae (14), (15) that is $\mathrm{i}\omega$, $\mathrm{i}\omega/c^2$ are not the usual ones obtained when the Maxwell equations are written for the electric and the magnetic fields as unknowns. In fact, we started from the Maxwell equations written for the electric field and the magnetic induction vector as unknowns (see (1), (2)). We note that for $\omega\in\mathbf{R}$, $\underline{\alpha}\in\partial B$ the vector $\underline{b}^s_{\omega,\underline{\alpha}}(\underline{x})$, is defined almost everywhere in $\underline{x}$ for $\underline{x}\in\partial\Omega$ and that equation (18), together with the time-harmonic Maxwell equations (14), (15), implies (7) and (8) when the integrals in (12), (13) are well-behaved. It is easy to see that, for $\omega\in\mathbf{R}$, $\underline{\alpha}\in\partial B$, (14–16), (18) imply that $\underline{E}^s_{\omega,\underline{\alpha}}$ satisfies the following exterior boundary-value problem:

$$(\mathbf{\Delta}\underline{E}^s_{\omega,\underline{\alpha}}+(\frac{\omega}{c})^2\underline{E}^s_{\omega,\underline{\alpha}})(\underline{x})=\underline{0},\quad \underline{x}\in\mathbf{R}^3\backslash\overline{\Omega}\,, \tag{19}$$

$$\mathrm{div}\underline{E}^s_{\omega,\underline{\alpha}}(x)=0,\quad \underline{x}\in\mathbf{R}^3\backslash\overline{\Omega}\,, \tag{20}$$

$$[\underline{n},\underline{E}^s_{\omega,\underline{\alpha}}](\underline{x})-\frac{\chi c}{\mathrm{i}\omega}[\underline{n},[\underline{n},\mathrm{curl}\underline{E}^s_{\omega,\underline{\alpha}}]](\underline{x})=[\underline{n},\underline{b}_{\omega,\underline{\alpha}}](\underline{x}),\ \underline{x}\in\partial\Omega, \tag{21}$$

$$[\mathrm{curl}\underline{E}^s_{\omega,\underline{\alpha}},\hat{\underline{x}}]-\mathrm{i}\frac{\omega}{c}\underline{E}^s_{\omega,\underline{\alpha}}=o\left(\frac{1}{r}\right),\quad r\to+\infty, \tag{22}$$

where ω/c is the wave number, $\mathbf{\Delta}$ denotes the Laplace operator $\Delta=\sum_{i=1}^3\partial^2/\partial x_i^2$ acting on each component of the vector $\underline{E}^s_{\omega,\underline{\alpha}}$, that is $\underline{E}^s_{\omega,\underline{\alpha}}=(E^s_{\omega,\underline{\alpha},1},E^s_{\omega,\underline{\alpha},2},E^s_{\omega,\underline{\alpha},3})^T$ and $\mathbf{\Delta}\underline{E}^s_{\omega,\underline{\alpha}}=(\Delta E^s_{\omega,\underline{\alpha},1},\Delta E^s_{\omega,\underline{\alpha},2},\Delta E^s_{\omega,\underline{\alpha},3})^T$.

Equation (19) is called vector Helmholtz equation. We note that when $\chi = \infty$, that is, when the obstacle is perfectly insulating, the boundary condition (21) can be rewritten, by dividing both sides by χ and using the fact that $1/\chi = 0$ when $\chi = \infty$. When $\chi = 0$, that is, when the obstacle is perfectly conducting, the boundary condition (21) makes sense for $\omega \in \mathbf{R}$. When $\chi \neq 0$ the boundary condition (21) makes sense for $\omega \neq 0$; in order to deal with the case $\omega = 0$, we multiply Equation (21) by ω when $\omega \neq 0$ and we note that the boundary condition obtained by multiplying (21) by ω makes sense, even when $\omega = 0$. Moreover, for $\omega \in \mathbf{R}$, $\underline{\alpha} \in \partial B$, when $\underline{E}^s_{\omega,\underline{\alpha}}$ is the solution of the exterior boundary-value problem (19–22) from (14), we have:

$$\underline{B}^s_{\omega,\underline{\alpha}}(\underline{x}) = -\frac{\mathrm{i}}{\omega}\mathrm{curl}\,\underline{E}^s_{\omega,\underline{\alpha}}(\underline{x}), \quad \underline{x} \in \mathbf{R}^3 \backslash \overline{\Omega}\,. \tag{23}$$

When necessary, the division by ω in (23) must be interpreted using the theory of distributions.

From now on we treat explicitly only the case $\chi \neq \infty$ and $\omega \neq 0$. The remaining cases can be treated analogously, and are omitted to keep the exposition simple.

3. The basic ideas of the method

Let us explain the basic ideas $(i1)$ and $(i2)$ of the method that we propose in this paper.

Let (r, θ, ϕ) be the canonical spherical coordinates in $\mathbf{R}^3$, for $\underline{\alpha} \in \partial B$ let $z = \cos\theta$, $0 \leq \theta \leq \pi$, we have:

$$\underline{\alpha}(z, \phi) = (\cos\phi \sin\cos^{-1} z, \sin\phi \sin\cos^{-1} z, z)^T, -1 \leq z \leq 1, 0 \leq \phi < 2\pi. \tag{24}$$

Let N_1, N_2, N_3 be three positive integers, $\underline{\omega}^{N_1} = (\omega_1, \omega_2, \ldots, \omega_{N_1})^T \in \mathbf{R}^{N_1}$, $\underline{\phi}^{N_2} = (\phi_1, \phi_2, \ldots, \phi_{N_2})^T \in \mathbf{R}^{N_2}$, $\underline{z}^{N_3} = (z_1, z_2, \ldots, z_{N_3})^T \in \mathbf{R}^{N_3}$, be such that (ω_i, ϕ_j, z_k), $i = 1, 2, \ldots, N_1$, $j = 1, 2, \ldots, N_2$, $k = 1, 2, \ldots, N_3$ are the nodes of a quadrature rule on $\mathbf{R} \times \partial B$, and let

$$\underline{\alpha}_{j,k} = (\cos\phi_j \sin\cos^{-1} z_k, \sin\phi_j \sin\cos^{-1} z_k, z_k)^T, \; j = 1, 2, \ldots, N_2, \quad k = 1, 2, \ldots, N_3. \tag{25}$$

Let $A \in \mathbf{R}^{N_1 \times N_2 \times N_3}$ be the multilinear transformation that contains the weights of the quadrature rule, that is $(A)_{i,j,k} = a_{i,j,k}$, $i = 1, 2, \ldots, N_1$, $j = 1, 2, \ldots, N_2$, $k = 1, 2, \ldots, N_3$, are the weights of the quadrature rule.

The basic idea $(i1)$ of the method is to approximate the integral appearing in (9), (10), and (12), (13) by a quadrature rule of the type described above, that is, we consider the following approximation for the scattered electromagnetic field:

$$\underline{\mathcal{E}}^s(\underline{x}, t) \approx \frac{1}{(2\pi)^4} \sum_{i=1}^{N_1} \sum_{j=1}^{N_2} \sum_{k=1}^{N_3} a_{i,j,k} \exp(-\mathrm{i}\omega_i t) \underline{E}^s_{\omega_i, \underline{\alpha}_{j,k}}(\underline{x}), \tag{26}$$

$$\underline{\mathcal{B}}^s(\underline{x}, t) \approx \frac{1}{(2\pi)^4} \sum_{i=1}^{N_1} \sum_{j=1}^{N_2} \sum_{k=1}^{N_3} a_{i,j,k} \exp(-\mathrm{i}\omega_i t) \underline{B}^s_{\omega_i, \underline{\alpha}_{j,k}}(\underline{x}). \tag{27}$$

Note that the choice of the quadrature formula (see (26), (27)) depends on the weight function w appearing in (9), (10) and (12), (13) when the remaining functions depending on ω in those integrals are well-behaved.

The second basic idea of the method $(i2)$ is the formulation of a new 'operator expansion method' to compute the solution $\underline{E}^s_{\omega,\underline{\alpha}}$ of the boundary-value problem (19–22) for $(\omega, \underline{\alpha}) = (\omega_i, \underline{\alpha}_{j,k})$, $i = 1, 2, \ldots, N_1$, $j = 1, 2, \ldots, N_2$, $k = 1, 2, \ldots, N_3$. From the knowledge of $\underline{E}^s_{\omega,\underline{\alpha}}$ the solution of the time-harmonic Maxwell equations (14), (15) is obtained using Equation (23).

Summing up, we approximate the solution of the time-dependent Maxwell equations (1–5), (7), (8) by the linear combination coming from the quadrature rule chosen from the solutions of the $N_1 \cdot N_2 \cdot N_3$ boundary-value problems for the time-harmonic Maxwell equations (14–16), (18) or equivalently (19–23). The time-harmonic exterior boundary-value problems considered are independent one from the other and can be solved in parallel, that is, condition $(r4)$ is fulfilled. Moreover, since the 'operator expansion' method is highly parallelizable, also the computation of each time-harmonic electromagnetic scattered field $\underline{E}^s_{\omega,\underline{\alpha}}(\underline{x})$, $\underline{B}^s_{\omega,\underline{\alpha}}(\underline{x})$, $(\omega, \underline{\alpha}) = (\omega_i, \underline{\alpha}_{j,k})$, $i = 1, 2, \ldots, N_1$, $j = 1, 2, \ldots, N_2$, $k = 1, 2, \ldots, N_3$, can be done efficiently in parallel.

Note that the integral representation formulae (12) and (13) in some sense imply the assumption of the Courant-Friedrichs and Levy stability condition on the space and time steps. Thanks to these representation formulae, the use of a suitable quadrature rule and the use of the 'operator expansion method', conditions $(r2)$ and $(r4)$ are fulfilled.

Now we give a detailed description of the 'operator expansion' method used.

The 'operator expansion' method used here is based on the following assumptions (see [21, Section 1]):
a) Ω is a bounded obstacle whose boundary is a starlike surface with respect to the origin, that is:

$$\Omega = \{\underline{x} = r\hat{\underline{x}} \in \mathbf{R}^3 |\ 0 \leq r < \xi(\hat{\underline{x}}), \quad \hat{\underline{x}} \in \partial B\}, \tag{28}$$

$$\partial\Omega = \{\underline{x} = r\hat{\underline{x}} \in \mathbf{R}^3 |\ r = \xi(\hat{\underline{x}}), \quad \hat{\underline{x}} \in \partial B\}, \tag{29}$$

where $\xi(\hat{\underline{x}}) > 0, \hat{\underline{x}} \in \partial B$ is a single-valued sufficiently regular function defined on ∂B.
b) For each $\omega \in \mathbf{R}$ there exists B_a with $0 < a = a(\omega) < 1$ such that $\Omega \supset \overline{B}_{a(\omega)}$, $\overline{\cup_{\omega\in\mathbf{R}} B_{a(\omega)}} \subset \Omega$ and the solution $\underline{E}^s_{\omega,\underline{\alpha}}$ of (19–22) defined for $\underline{x} \in \mathbf{R}^3 \backslash \overline{\Omega}$ can be extended to $\underline{x} \in \mathbf{R}^3 \setminus \overline{B}_{a(\omega)}$ remaining a divergence-free vector-field solution of the vector Helmholtz equation in $\mathbf{R}^3 \setminus \overline{B}_{a(\omega)}$. We denote this extension of $\underline{E}^s_{\omega,\underline{\alpha}}(\underline{x})$ with $\underline{F}_{\omega,\underline{\alpha}}(\underline{x})$, and we assume that $\underline{F}_{\omega,\underline{\alpha}}(\underline{x})$ can be represented as follows:

$$\underline{F}_{\omega,\underline{\alpha}}(\underline{x}) = a^2 \mathrm{curl}_{\underline{x}} \int_{\partial B} \Phi_\omega(\underline{x}, a\hat{\underline{y}}) \underline{v}_{\omega,\underline{\alpha}}(\hat{\underline{y}}) \mathrm{d}s(\hat{\underline{y}}), \underline{x} \in \mathbf{R}^3 \backslash \overline{B}_a\,, \tag{30}$$

where, to avoid confusion, we write $\mathrm{curl}_{\underline{x}}$ to mean the curl operator with respect to the $\underline{x}$ variable, $\underline{v}_{\omega,\underline{\alpha}}(\hat{\underline{y}})$ is a suitable vector-density function and finally:

$$\Phi_\omega(\underline{x}, \underline{y}) = \frac{e^{\mathrm{i}\frac{\omega}{c}\|\underline{x}-\underline{y}\|}}{4\pi\|\underline{x}-\underline{y}\|}\,, \underline{x} \neq \underline{y}\,, \tag{31}$$

is the fundamental solution of the Helmholtz equation in $\mathbf{R}^3$ with the Sommerfeld radiation condition at infinity.

The previous assumptions a) and b) are sufficient conditions to develop the operator-expansion method. The operator-expansion method can be developed under more general conditions. We note that, for any choice of $\underline{v}_{\omega,\underline{\alpha}}$ that enables us to differentiate under the

integral sign in (30), we have that the vector field $\underline{F}_{\omega,\underline{\alpha}}(\underline{x})$ in (30) is a divergence-free vector-field solution of the vector Helmholtz equation for $\underline{x} \in \mathbf{R}^3 \backslash \overline{B}_a$ so that $\underline{F}_{\omega,\underline{\alpha}}(\underline{x})$ satisfies (19), (20); moreover $\underline{F}_{\omega,\underline{\alpha}}(\underline{x})$ satisfies the radiation condition at infinity (22), *i.e.*, condition $(r1)$ is satisfied.

We determine the vector density function $\underline{v}_{\omega,\underline{\alpha}}(\underline{\hat{y}})$ appearing in (30) by imposing the boundary condition (21), that is, imposing that $\underline{F}_{\omega,\underline{\alpha}}(\underline{x})$ extends $\underline{E}^s_{\omega,\underline{\alpha}}(\underline{x})$ and we solve the resulting integral equation using a formal power-series expansion with respect to $\|\underline{x}\|$ having $\partial B = \{\underline{x} \in \mathbf{R}^3 |\ \|\underline{x}\| = 1\}$ as base point (see Section 4). This is the 'operator expansion' method. Moreover, as shown in Section 5 (see formulae (56), (57)), the coefficients of the series expansion of $\underline{F}_{\omega,\underline{\alpha}}(\underline{x})$ in powers of $\|\underline{x}\| - 1$ are independent of the choice of the radius a of the sphere B_a.

We conclude this section noting that the proposed method allows us to solve many different problems. In particular, in the numerical experiments shown in Section 6, we use the numerical method proposed to solve problem (1–5), (7), (8) in two particular cases. That is, we consider the following two electromagnetic incident fields:

$$\underline{\mathcal{E}}^i(\underline{x}, t) = \underline{P} \exp(\mathrm{i}\frac{\omega^*}{c}[(\underline{\gamma}, \underline{x}) - ct]),\ (\underline{x}, t) \in \mathbf{R}^3 \times \mathbf{R}, \tag{32}$$

$$\underline{\mathcal{B}}^i(\underline{x}, t) = \frac{1}{c}[\underline{\gamma}, \underline{P}] \exp(\mathrm{i}\frac{\omega^*}{c}[(\underline{\gamma}, \underline{x}) - ct]),\ (\underline{x}, t) \in \mathbf{R}^3 \times \mathbf{R}, \tag{33}$$

and

$$\underline{\mathcal{E}}^i(\underline{x}, t) = \underline{P} \exp(-\frac{1}{4\zeta^2}[(\underline{\gamma}, \underline{x}) - ct]^2),\ (\underline{x}, t) \in \mathbf{R}^3 \times \mathbf{R}, \tag{34}$$

$$\underline{\mathcal{B}}^i(\underline{x}, t) = \frac{1}{c}[\underline{\gamma}, \underline{P}] \exp(-\frac{1}{4\zeta^2}[(\underline{\gamma}, \underline{x}) - ct]^2),\ (\underline{x}, t) \in \mathbf{R}^3 \times \mathbf{R}, \tag{35}$$

where $\underline{\gamma} \in \partial B$ is a given vector, ω^*, $\zeta > 0$ are given constants, and $\underline{P} \in \mathbf{R}^3$ is a given vector such that:

$$(\underline{P}, \underline{\gamma}) = 0. \tag{36}$$

The incident electromagnetic field (32), (33) is the field associated with a time-harmonic linearly polarized incoming plane wave, the vector $\underline{\gamma}$ is the propagation direction and $\underline{P}$ is the polarization vector of the incident electric field. We note that in this case in formula (9) we can choose $\underline{V}(\omega, \underline{\alpha}) = (2\pi)^4 \underline{P}\delta(\underline{\alpha} - \underline{\gamma})\delta(\omega - \omega^*)$, $w(\omega) = 1$, where δ is the 'Dirac's delta' function. With abuse of notation we denote by δ the 'Dirac's delta' function on $\mathbf{R}^3$, or on $\mathbf{R}$, or on ∂B.

In the case (34), (35) in formula (9) we can choose $\underline{V}(\omega, \underline{\alpha}) = ((2\pi)^4/\sqrt{\pi})\underline{P}\delta(\underline{\alpha} - \underline{\gamma})$ and $w(\omega) = \zeta \exp(-\zeta^2\omega^2)$, and the incoming electromagnetic field is a linear superposition of time-harmonic plane waves propagating in the direction $\underline{\gamma}$ with polarization vector $\underline{P}$.

In the numerical experiments shown in Section 6, when we choose the electromagnetic incident field to be given by (32), (33) in formulae (12), (13), there are no integrals to compute, that is, no quadrature rule is needed. When we choose the incident field to be given by (34), (35), the integrals (9), (10), (12), (13) reduce to one-dimensional integrals in the variable ω with $w(\omega) = \zeta \exp(-\zeta^2\omega^2)$, that is, only the integral in the variable ω must be computed by numerical quadrature.

We make this choice of the weight function, since it is a natural one due to the particular form of the Fourier transform of the electromagnetic incident field (34), (35). In fact, since we have $w(\omega) = \zeta \exp(-\zeta^2\omega^2)$, $\zeta > 0$, $\omega \in \mathbf{R}$, we use the Gauss-Hermite quadrature rule to compute the integrals in the ω variable, and we compute the solution $\underline{E}^s_{\omega,\underline{\alpha}}$ of the boundary-value problem (19–22) with $\underline{\alpha} = \underline{\gamma}$ and $\omega = \omega_i$, $i = 1, 2, \ldots, N_1$ via the 'operator expansion' method. We note that for these two classes of incident electromagnetic fields we can choose $N_2 = N_3 = 1$ with great savings in computer time.

Furthermore, we note that the method proposed can be applied also when the incident field includes evanescent waves. In this case a large number of time-harmonic electromagnetic fields must be used in order to get a satisfactory approximation of the incident field in a compact region surrounding the obstacle. However, probably in this case representation formulae more appropriate than formulae (9) and (10), that is, more appropriate than expansions in plane waves, can be considered.

4. The expansion of the time-harmonic electromagnetic field

In this section we solve the exterior boundary-value problem for the vector Helmholtz equation (19–22) for a given value of the wave number $(\frac{\omega}{c}) \neq 0$ and for a given propagation direction $\underline{\alpha} \in \partial B$ of the incoming time-harmonic linearly polarized electromagnetic plane wave. We note that, when $\frac{\omega}{c} = 0$ and χ is a finite nonzero constant, we have $\underline{E}_{0,\underline{\alpha}}(\underline{x}) \equiv 0$, $\underline{\alpha} \in \partial B$. When $\frac{\omega}{c} = 0$ and $\chi = \infty$ or $\chi = 0$, the boundary condition (21) must be changed as discussed in Section 2 and $\underline{E}_{0,\underline{\alpha}}(\underline{x})$ will not be equal to zero in general. Now let χ be a finite nonzero constant, $0 < a < 1$, B_a and $\partial\Omega$ be as specified in Section 3; in particular, let us assume that $\overline{B}_a \subset \Omega$ and that (29) holds. We take $a < 1$ since we want to be able to choose $\Omega = B$. We assume that the solution $\underline{E}^s_{\omega,\underline{\alpha}}$ of the exterior boundary-value problem (19–22), can be extended to $\underline{x} \in \mathbf{R}^3 \backslash \overline{B}_a$ remaining a divergence-free vector-field solution of the vector Helmholtz equation in $\mathbf{R}^3 \backslash \overline{B}_a$ and that this extension $\underline{F}_{\omega,\underline{\alpha}}(\underline{x})$ is given by formula (30), where we assume that the density $\underline{v}_{\omega,\underline{\alpha}}(\underline{\hat{y}})$ is tangential to ∂B, that is:

$$(\underline{v}_{\omega,\underline{\alpha}}(\underline{\hat{y}}), \underline{\hat{y}}) = 0\,, \quad \underline{\hat{y}} \in \partial B\,. \tag{37}$$

We note that condition $(r1)$ is fulfilled and that condition (37) is required to determine uniquely the vector-density function $\underline{v}_{\omega,\underline{\alpha}}(\underline{\hat{y}})$. In fact, as we will show in Section 5, the component of the vector-density function $\underline{v}_{\omega,\underline{\alpha}}(\underline{\hat{y}})$ in the radial direction $\underline{\hat{x}} \in \partial B$ is not uniquely determined by the condition that $\underline{F}_{\omega,\underline{\alpha}}(\underline{x})$ is an extension of $\underline{E}^s_{\omega,\underline{\alpha}}(\underline{x})$. With abuse of notation, when $\underline{v}_{\omega,\underline{\alpha}}$ is a complex vector-valued function in Equation (37), the scalar product must be interpreted as the real Euclidean scalar product of complex vectors.

We note that for any choice of the vector-density function $\underline{v}_{\omega,\underline{\alpha}}$ that makes possible differentiation under the integral sign in (30) we have that $\underline{F}_{\omega,\underline{\alpha}}$ satisfies Equations (19) and (20) in $\mathbf{R}^3 \backslash \overline{B}_a$ and the radiation condition at infinity (22).

We determine $\underline{v}_{\omega,\underline{\alpha}}$ by imposing that $\underline{F}_{\omega,\underline{\alpha}}$ extends $\underline{E}^s_{\omega,\underline{\alpha}}$, that is, imposing the boundary condition (21):

$$[\underline{n}, \underline{F}_{\omega,\underline{\alpha}}](\underline{x}) - \frac{\chi c}{\mathrm{i}\omega}[\underline{n}, [\underline{n}, \operatorname{curl}_{\underline{x}} \underline{F}_{\omega,\underline{\alpha}}]](\underline{x}) = [\underline{n}, \underline{b}_{\omega,\underline{\alpha}}](\underline{x}),\ \underline{x} \in \partial\Omega, \tag{38}$$

where $\underline{b}_{\omega,\underline{\alpha}}$ is the vector field given by (17). We note that, when $\partial\Omega$ is only a locally Lipschitz surface, Equation (38) holds only almost everywhere in $\underline{x}$ for $\underline{x} \in \partial\Omega$ (see [34, Lemma 2.42,

p. 88]). Equation (38) can be viewed as a linear integral equation in the unknown $\underline{v}_{\omega,\underline{\alpha}}$. This is the integral equation discussed in Section 1 that we want to solve with the 'operator expansion' method. That is, we solve Equation (38) using a perturbative series with base point $\partial B = \{\, \underline{x} \in \mathbf{R}^3 \mid \|\underline{x}\| = 1 \,\}$; in particular, we assume that the following formal series expansion for the vector density $\underline{v}_{\omega,\underline{\alpha}}(\hat{\underline{y}})$ holds:

$$\underline{v}_{\omega,\underline{\alpha}}(\hat{\underline{y}}) = \sum_{s=0}^{+\infty} \frac{(\xi(\hat{\underline{y}}) - 1)^s}{s!} \underline{v}_{\omega,\underline{\alpha},s}(\hat{\underline{y}}), \quad \hat{\underline{y}} \in \partial B\,, \tag{39}$$

where we assume $0! = 1$ and the 'coefficients' of the expansion $\underline{v}_{\omega,\underline{\alpha},s}(\hat{\underline{y}})$, $\hat{\underline{y}} \in \partial B$, $s = 0, 1, \ldots$ are vector fields tangential to ∂B to be determined. That is, Equation (37) holds order by order in the expansion in powers of $(\xi - 1)$.

In the following with abuse of notation we use ξ as an independent variable so that the notation $O((\xi - 1)^\nu)$, $\nu \geq 0$ when $\xi \to 1$ is a meaningful notation.

From now on we take $\mathrm{curl}_{\underline{x}}$ and $\frac{\partial}{\partial \|\underline{x}\|}$ outside and inside of the integral signs as needed, that is, we assume that the integrals are sufficiently well-behaved to make these operations legitimate.

Let $\underline{e}(\hat{\underline{x}})$, $\hat{\underline{x}} \in \partial B$ be an absolutely integrable vector function with respect to the surface measure defined on ∂B and tangential to ∂B, that is:

$$(\underline{e}(\hat{\underline{x}}) = 0, \quad \hat{\underline{x}} \in \partial B\,; \tag{40}$$

for $0 < a < 1$ we define the operators $p_{\omega,s}$, $q_{\omega,s}$, $s = 0, 1, \ldots$, as follows:

$$(p_{\omega,s}\underline{e})(\underline{x}) = a^2 \int_{\partial B} \frac{\partial^s}{\partial \|\underline{x}\|^s} \mathrm{curl}_{\underline{x}} \Phi_\omega(\underline{x}, a\hat{\underline{y}}) \underline{e}(\hat{\underline{y}}) \mathrm{d}s(\hat{\underline{y}}), \qquad \|\underline{x}\| > a,\ s = 0, 1, \ldots, \tag{41}$$

$$(q_{\omega,s}\underline{e})(\underline{x}) = a^2 \int_{\partial B} \frac{\partial^s}{\partial \|\underline{x}\|^s} \mathrm{curl}_{\underline{x}} \mathrm{curl}_{\underline{x}} \Phi_\omega(\underline{x}, a\hat{\underline{y}}) \underline{e}(\hat{\underline{y}}) \mathrm{d}s(\hat{\underline{y}}), \qquad \|\underline{x}\| > a,\ s = 0, 1, \ldots, \tag{42}$$

and the operators $\hat{p}_{\omega,s}$, $\hat{q}_{\omega,s}$, are defined as follows:

$$(\hat{p}_{\omega,s}\underline{e})(\hat{\underline{x}}) = (p_{\omega,s}\underline{e})(\hat{\underline{x}}), \quad \hat{\underline{x}} \in \partial B, s = 0, 1, \ldots\,, \tag{43}$$

$$(\hat{q}_{\omega,s}\underline{e})(\hat{\underline{x}}) = (q_{\omega,s}\underline{e})(\hat{\underline{x}}), \quad \hat{\underline{x}} \in \partial B, s = 0, 1, \ldots\,. \tag{44}$$

Finally we define the operator $\hat{l}_\omega$ that maps tangential vector fields defined on ∂B into tangential vector fields defined on ∂B via the following equation:

$$[\hat{\underline{x}}, (\hat{p}_{\omega,0}(\hat{l}_\omega \underline{e}))(\hat{\underline{x}})] - \chi \frac{c}{\mathrm{i}\omega} [\hat{\underline{x}}, [\hat{\underline{x}}, (\hat{q}_{\omega,0}(\hat{l}_\omega \underline{e}))(\hat{\underline{x}})]] = \underline{e}(\hat{\underline{x}}), \hat{\underline{x}} \in \partial B, \tag{45}$$

where $\hat{p}_{\omega,0}$, $\hat{q}_{\omega,0}$ are the operators defined in (43), (44) with $s = 0$. We can prove that the following relations hold:

$$\frac{(\xi - 1)^s}{s!} \underline{v}_{\omega,\alpha,s}(\hat{\underline{x}}) = (\hat{l}_\omega \underline{z}_{\omega,\underline{\alpha},s})(\hat{\underline{x}}),\ s = 0, 1, \ldots, \hat{\underline{x}} \in \partial B,\ \omega \in \mathbf{R},\ \underline{\alpha} \in \partial B, \tag{46}$$

where the vector fields $\underline{z}_{\omega,\underline{\alpha},s}$, $s = 0, 1, \ldots$, are defined by recursion from the datum $\underline{b}_{\omega,\underline{\alpha}}(\underline{x})$, $\underline{x} \in \partial\Omega$ imposing that Equation (38) holds order by order in powers of $(\xi - 1)$.

Note that Equation (45) leaves undetermined the radial component of the unknown vector field $\hat{l}_\omega \underline{e}$, so that, by imposing that $\hat{l}_\omega \underline{e}$ is a tangential vector field to ∂B, we choose this

component to be equal zero. We note that Equation (45) coincides with Equation (38) when $\partial\Omega = \partial B$ and that in (38) we have $\underline{e}(\underline{\hat{x}}) = [\underline{\hat{x}}, \underline{b}_{\omega,\underline{\alpha}}(\underline{\hat{x}})]$, $\underline{\hat{x}} \in \partial B$, where $\underline{b}_{\omega,\underline{\alpha}}$ is given by (17). We note that Equation (45) holds on ∂B. This fact and the character of the operators $\hat{p}_{\omega,0}$, $\hat{q}_{\omega,0}$, makes possible to reduce the solution of (45) to the solution of an 'easy' linear system by choosing appropriately the basis used to represent the integral operators $\hat{p}_{\omega,0}$, $\hat{q}_{\omega,0}$ (see Section 5). The basis to be chosen is the basis of the vector spherical harmonics; a similar simple choice is not possible when we approximate the integrals in (38) by finite sums or when ∂B_a is not chosen as reference surface in (30) and ∂B is not chosen as base point of the power-series expansion. From formulae (30) and (46), using the expansion (39), the expansions of $\mathrm{curl}_{\underline{x}}\{\Phi_\omega(\underline{x}, a\underline{\hat{y}})\underline{v}_{\omega,\underline{\alpha}}(\underline{\hat{y}})\}$ and of $\mathrm{curl}_{\underline{x}}\mathrm{curl}_{\underline{x}}\{\Phi_\omega(\underline{x}, a\underline{\hat{y}})\underline{v}_{\omega,\underline{\alpha}}(\underline{\hat{y}})\}$ in powers of $(\|\underline{x}\| - 1)$ and the Cauchy product rule between series, we have:

$$\underline{F}_{\omega,\underline{\alpha}}(\underline{x}) = \sum_{s=0}^{+\infty}\sum_{l=0}^{s}\frac{(\|\underline{x}\|-1)^{s-l}}{(s-l)!}\left(\hat{p}_{\omega,s-l}(\hat{l}_\omega \underline{z}_{\omega,\underline{\alpha},l})\right)(\underline{\hat{x}})\,,\ \underline{x} \in \mathbf{R}^3\backslash\overline{B}_a\,, \tag{47}$$

and

$$\mathrm{curl}_{\underline{x}}\underline{F}_{\omega,\underline{\alpha}}(\underline{x}) = \sum_{s=0}^{+\infty}\sum_{l=0}^{s}\frac{(\|\underline{x}\|-1)^{s-l}}{(s-l)!}\left(\hat{q}_{\omega,s-l}(\hat{l}_\omega \underline{z}_{\omega,\underline{\alpha},l})\right)(\underline{\hat{x}})\,,\ \underline{x} \in \mathbf{R}^3\backslash\overline{B}_a\,. \tag{48}$$

Note that the vector fields $\underline{F}_{\omega,\underline{\alpha}}(\underline{x})$ and $\mathrm{curl}_{\underline{x}}\underline{F}_{\omega,\underline{\alpha}}(\underline{x})$ are known when the vector functions $(\hat{p}_{\omega,s-\nu}(\hat{l}_\omega \underline{z}_{\omega,\underline{\alpha},\nu}))(\underline{\hat{x}})$, $(\hat{q}_{\omega,s-\nu}(\hat{l}_\omega \underline{z}_{\omega,\underline{\alpha},\nu}))(\underline{\hat{x}})$, $\underline{\hat{x}} \in \partial B$, $s = 0, 1, \ldots$, $\nu = 0, 1, \ldots, s$ are determined. In the hypotheses specified previously when $|\xi(\underline{\hat{x}}) - 1|$, $\underline{\hat{x}} \in \partial B$ is sufficiently small, we have that the series (39), converges, that is, formulae (47) and (48) hold.

5. The computational method

Let $L^2(\partial B)$ be the space of square integrable functions with respect to the surface measure defined on ∂B, and let $\{\underline{B}_{\sigma,m,l}(\underline{\hat{x}}), \underline{C}_{\sigma,m,l}(\underline{\hat{x}}), \underline{P}_{\sigma,m,l}(\underline{\hat{x}})\}_{\sigma=0,1,\, l=\sigma,\sigma+1,\ldots,\, m=\sigma,\ldots,l}$, $\underline{\hat{x}} \in \partial B$ be the complete orthonormal set of $(L^2(\partial B))^3$ made of the vector spherical harmonic functions (see [39, Chp. 13, p. 1898]); in this section we give a simple expansion with respect to this basis of the vector field $\underline{F}_{\omega,\underline{\alpha}}(\underline{x})$ defined in formula (30). We show that the use of this basis allows us to represent the operators $\hat{p}_{\omega,s}$, $\hat{q}_{\omega,s}$, $s = 0, 1, \ldots$, $\hat{l}_\omega$ by simple infinite matrices.

Let $h_l(y)$, $j_l(y)$, $y \in \mathbf{C}$, $l = 0, 1, 2, \ldots$ be the spherical Hankel and the spherical Bessel functions, respectively, and let $h_l^{(\nu)}(y) = \mathrm{d}^\nu h_l(y)/\mathrm{d}y^\nu$, $y \in \mathbf{C}$, $\nu = 0, 1, \ldots$, $l = 0, 1, \ldots$; we define the following quantities:

$$r_{\omega,s,l} = (\frac{\omega}{c})^s \sum_{\nu=0}^{s}\frac{s!}{(s-\nu)!}(-1)^\nu \frac{h_l^{(s-\nu)}(\frac{\omega}{c})}{(\frac{\omega}{c})^{\nu+1}},\ \omega \in \mathbf{R},\ s = 0, 1, \ldots,\ l = 0, 1, \ldots\,, \tag{49}$$

$$d_{\omega,1,l} = ((l+1)h_l(\frac{\omega}{c}) - \frac{\omega}{c}h_{l+1}(\frac{\omega}{c})) - \frac{\chi}{\mathrm{i}}\frac{\omega}{c}h_l(\frac{\omega}{c}),\ \omega \in \mathbf{R},\ l = 0, 1, \ldots\,, \tag{50}$$

and finally:

$$d_{\omega,2,l} = h_l(\frac{\omega}{c}) + \frac{\chi c}{\mathrm{i}\omega}((l+1)h_l(\frac{\omega}{c}) - \frac{\omega}{c}h_{l+1}(\frac{\omega}{c})),\ \omega \in \mathbf{R},\ l = 0, 1, \ldots\,. \tag{51}$$

It is easy to see ([38, p. 439]) that when $\chi \geq 0$ we have:

$$d_{\omega,1,l} \neq 0, \quad d_{\omega,2,l} \neq 0, \omega \in \mathbf{R},\ l = 0, 1, \ldots . \tag{52}$$

Let $\underline{e}$ be a locally integrable vector field defined on ∂B and tangential to ∂B, *i.e.*, Equation (40) holds, then the following expansion of $\underline{e}$ holds:

$$\underline{e}(\underline{\hat{x}}) = \sum_{\sigma=0}^{1}\sum_{l=1}^{+\infty}\sum_{m=\sigma}^{l}\{e_{C_{\sigma,m,l}}\underline{C}_{\sigma,m,l}(\underline{\hat{x}}) + e_{B_{\sigma,m,l}}\underline{B}_{\sigma,m,l}(\underline{\hat{x}})\},\ \underline{\hat{x}} \in \partial B, \tag{53}$$

where $\{e_{C_{\sigma,m,l}}, e_{B_{\sigma,m,l}}\}$, $\sigma = 0, 1$, $l = 1, 2, \ldots$, $m = \sigma, \sigma+1, \ldots, l$ are the generalized Fourier coefficients of $\underline{e}$ with respect to the basis of vector spherical harmonics. Let the operators $\hat{p}_{\omega,s}$, $\hat{q}_{\omega,s}$, $s = 0, 1, 2, \ldots$, $\hat{l}_\omega$ be given by (43), (44), (45), with an involved but elementary computation using the free space Green's dyadic formula (see [39, Chapter 13, p. 1875]) we obtain:

$$\begin{aligned}(\hat{p}_{\omega,s}(\hat{l}_\omega(\underline{e}))(\underline{\hat{x}}) = \sum_{\sigma=0}^{1}\sum_{l=1}^{+\infty}\sum_{m=\sigma}^{l}\Bigg\{&-\frac{\underline{P}_{\sigma,m,l}(\underline{\hat{x}})e_{C_{\sigma,m,l}}(\frac{\omega}{c})\sqrt{l(l+1)}r_{\omega,s,l}}{d_{\omega,1,l}}\\ +\frac{\underline{C}_{\sigma,m,l}(\underline{\hat{x}})e_{B_{\sigma,m,l}}(\frac{\omega}{c})^s h_l^{(s)}(\frac{\omega}{c})}{d_{\omega,2,l}} &- \frac{\underline{B}_{\sigma,m,l}(\underline{\hat{x}})e_{C_{\sigma,m,l}}(\frac{\omega}{c})\left((l+1)r_{\omega,s,l} - (\frac{\omega}{c})^s h_{l+1}^{(s)}(\frac{\omega}{c})\right)}{d_{\omega,1,l}}\Bigg\},\\ s = 0, 1, \ldots, \quad \underline{\hat{x}} \in \partial B,\end{aligned} \tag{54}$$

$$\begin{aligned}(\hat{q}_{\omega,s}(\hat{l}_\omega\underline{e}))(\underline{\hat{x}}) = \sum_{\sigma=0}^{1}\sum_{l=1}^{+\infty}\sum_{m=\sigma}^{l}\Bigg\{&\frac{\underline{P}_{\sigma,m,l}(\underline{\hat{x}})e_{B_{\sigma,m,l}}(\frac{\omega}{c})\sqrt{l(l+1)}r_{\omega,s,l}}{d_{\omega,2,l}} -\\ \frac{\underline{C}_{\sigma,m,l}(\underline{\hat{x}})e_{C_{\sigma,m,l}}(\frac{\omega}{c})^{s+2}h_l^{(s)}(\frac{\omega}{c})}{d_{\omega,1,l}} &+ \frac{\underline{B}_{\sigma,m,l}(\underline{\hat{x}})e_{B_{\sigma,m,l}}(\frac{\omega}{c})\left((l+1)r_{\omega,s,l} - (\frac{\omega}{c})^s h_{l+1}^{(s)}(\frac{\omega}{c})\right)}{d_{\omega,2,l}}\Bigg\},\\ s = 0, 1, \ldots, \quad \underline{\hat{x}} \in \partial B.\end{aligned} \tag{55}$$

We note that, when ω goes to zero, the operators in (54), (55) are well-defined and non-zero, since the limits $\lim_{\omega\to 0}\omega^\nu h_l^{(\nu)}(\omega/c)/h_l(\omega/c)$, $\nu = 0, 1, \ldots$, $l = 1, 2, \ldots$, are finite and not zero. Moreover, using the free space Green's dyadic formula, we get the following expansions in vector spherical harmonics of the vector field $\underline{F}_{\omega,\underline{\alpha},s}(\underline{x})$, $\underline{x} \in \mathbf{R}^3\backslash\overline{B}_a$, and of its curl:

$$\begin{aligned}\underline{F}_{\omega,\underline{\alpha}}(\underline{x}) = \sum_{s=0}^{+\infty}\sum_{\sigma=0}^{1}\sum_{l=1}^{+\infty}\sum_{m=\sigma}^{l}\Bigg\{&-\underline{P}_{\sigma,m,l}(\underline{\hat{x}})z_{\omega,\underline{\alpha},s,C_{\sigma,m,l}}\frac{\sqrt{l(l+1)}h_l((\frac{\omega}{c})\|\underline{x}\|)}{\|\underline{x}\|d_{\omega,1,l}} + \underline{C}_{\sigma,m,l}(\underline{\hat{x}})z_{\omega,\underline{\alpha},s,B_{\sigma,m,l}}\frac{h_l((\frac{\omega}{c})\|\underline{x}\|)}{d_{\omega,2,l}}\\ -\underline{B}_{\sigma,m,l}(\underline{\hat{x}})z_{\omega,\underline{\alpha},s,C_{\sigma,m,l}}&\frac{(l+1)h_l((\frac{\omega}{c})\|\underline{x}\|) - (\frac{\omega}{c})\|\underline{x}\|h_{l+1}((\frac{\omega}{c})\|\underline{x}\|)}{\|\underline{x}\|d_{\omega,1,l}}\Bigg\},\ \underline{x} = \|\underline{x}\|\underline{\hat{x}},\ \underline{\hat{x}} \in \partial B,\ \|\underline{x}\| > a,\end{aligned} \tag{56}$$

and

$$\begin{aligned}\mathrm{curl}_{\underline{x}}\underline{F}_{\omega,\underline{\alpha}}(\underline{x}) = \sum_{s=0}^{+\infty}\sum_{\sigma=0}^{1}\sum_{l=1}^{+\infty}\sum_{m=\sigma}^{l}\Bigg\{&\underline{P}_{\sigma,m,l}(\underline{\hat{x}})z_{\omega,\underline{\alpha},s,B_{\sigma,m,l}}\frac{\sqrt{l(l+1)}h_l((\frac{\omega}{c})\|\underline{x}\|)}{\|\underline{x}\|d_{\omega,2,l}} - \underline{C}_{\sigma,m,l}(\underline{\hat{x}})z_{\omega,\underline{\alpha},s,C_{\sigma,m,l}}\frac{(\frac{\omega}{c})^2 h_l((\frac{\omega}{c})\|\underline{x}\|)}{d_{\omega,1,l}}\\ +\underline{B}_{\sigma,m,l}(\underline{\hat{x}})z_{\omega,\underline{\alpha},s,B_{\sigma,m,l}}&\frac{(l+1)h_l((\frac{\omega}{c})\|\underline{x}\|) - (\frac{\omega}{c})\|\underline{x}\|h_{l+1}((\frac{\omega}{c})\|\underline{x}\|)}{\|\underline{x}\|d_{\omega,2,l}}\Bigg\},\ \underline{x} = \|\underline{x}\|\underline{\hat{x}},\ \underline{\hat{x}} \in \partial B,\ \|\underline{x}\| > a,\end{aligned} \tag{57}$$

where $z_{\omega,\underline{\alpha},s,C_{\sigma,m,l}}$, $z_{\omega,\underline{\alpha},s,B_{\sigma,m,l}}$ are the generalized Fourier coefficients of $\underline{z}_{\omega,\underline{\alpha},s}$, that is the vector field appearing in (46).

Note that for every fixed value of $s \geq 0$, $\omega \in \mathbf{R}$, $\underline{\alpha} \in \partial B$, the generalized Fourier coefficients $z_{\omega,\underline{\alpha},s,C_{\sigma,m,l}} = \int_{\partial B}(\underline{z}_{\omega,\underline{\alpha},s}(\underline{\hat{x}}), \underline{C}_{\sigma,m,l}(\underline{\hat{x}}))\mathrm{d}s(\underline{\hat{x}})$, $z_{\omega,\underline{\alpha},s,B_{\sigma,m,l}} = \int_{\partial B}(\underline{z}_{\omega,\underline{\alpha},s}(\underline{\hat{x}}), \underline{B}_{\sigma,m,l}(\underline{\hat{x}}))\mathrm{d}s(\underline{\hat{x}})$ $\sigma = 0, 1$, $l = 1, 2, \ldots$, $m = \sigma, \sigma+1, \ldots, l$ are double integrals independent one from the other so that they can be computed in parallel.

Let N_1, N_2, N_3 be positive integers, $\underline{\omega}^{N_1}$, $\underline{\phi}^{N_2}$, $\underline{z}^{N_3}$ be as specified in Section 3 and $\underline{\alpha}_{j,k}$, $j = 1, 2, \ldots, N_2$, $k = 1, 2, \ldots, N_3$, be given by (25), let $L_{\max} > 0$ be a positive integer, let $z_{\omega,\underline{\alpha},s,C_{\sigma,m,l}}$, $z_{\omega,\underline{\alpha},s,B_{\sigma,m,l}}$, $s = 0, 1, \ldots$, $\sigma = 0, 1$, $l = 1, \ldots, L_{\max}$, $m = \sigma, \ldots, l$ be given by (56), and finally let S be a positive integer. Using formulae (54), (55) into formulae (47), (45), we can approximate the scattered electromagnetic field $\underline{\mathcal{E}}^s$, $\underline{\mathcal{B}}^s$ with the following vector fields, respectively:

$$\underline{\mathcal{V}}^{S,N_1,N_2,N_3}_{L_{\max}}(\underline{x},t) = \frac{1}{(2\pi)^4}\sum_{i=1}^{N_1}\exp(-\mathrm{i}\omega_i t)\sum_{j=1}^{N_2}\sum_{k=1}^{N_3} a_{i,j,k}\underline{F}^{S,L_{\max}}_{\omega_i,\underline{\alpha}_{j,k}}(\underline{x}),\ (\underline{x},t) \in (\mathbf{R}^3 \setminus \overline{\Omega}) \times \mathbf{R}\,, \tag{58}$$

$$\underline{\mathcal{U}}^{S,N_1,N_2,N_3}_{L_{\max}}(\underline{x},t) = \frac{1}{(2\pi)^4}\sum_{i=1}^{N_1}\exp(-\mathrm{i}\omega_i t)\sum_{j=1}^{N_2}\sum_{k=1}^{N_3} a_{i,j,k}\mathrm{curl}_{\underline{x}}\underline{F}^{S,L_{\max}}_{\omega_i,\underline{\alpha}_{j,k}}(\underline{x}),\ (\underline{x},t) \in (\mathbf{R}^3 \setminus \overline{\Omega}) \times \mathbf{R}\,, \tag{59}$$

where $\underline{F}^{S,L_{\max}}_{\omega,\underline{\alpha}}(\underline{x})$ is the series given in (56) truncated at the S-th order:

$$\begin{aligned}\underline{F}^{S,L_{\max}}_{\omega,\underline{\alpha}}(\underline{x}) = \sum_{s=0}^{S}\sum_{\sigma=0}^{1}\sum_{l=1}^{L_{\max}}\sum_{m=\sigma}^{l}\Bigg\{&-\underline{B}_{\sigma,m,l}(\underline{\hat{x}})z_{\omega,\underline{\alpha},s,C_{\sigma,m,l}}\frac{(l+1)h_l((\frac{\omega}{c})\|\underline{x}\|) - (\frac{\omega}{c})\|\underline{x}\|h_{l+1}((\frac{\omega}{c})\|\underline{x}\|)}{\|\underline{x}\|d_{\omega,1,l}} - \\ &-\underline{P}_{\sigma,m,l}(\underline{\hat{x}})z_{\omega,\underline{\alpha},s,C_{\sigma,m,l}}\frac{\sqrt{l(l+1)}h_l((\frac{\omega}{c})\|\underline{x}\|)}{\|\underline{x}\|d_{\omega,1,l}} + \underline{C}_{\sigma,m,l}(\underline{\hat{x}})z_{\omega,\underline{\alpha},s,B_{\sigma,m,l}}\frac{h_l((\frac{\omega}{c})\|\underline{x}\|)}{d_{\omega,2,l}}\Bigg\}\,,\end{aligned} \tag{60}$$

$$\underline{\alpha} \in \partial B, \omega \in \mathbf{R}, \underline{x} = \|\underline{x}\|\underline{\hat{x}},\ \underline{\hat{x}} \in \partial B,\ \ \|\underline{x}\| > a.$$

6. Numerical results

We present some numerical results obtained by applying the computational method described in Sections 3–5 to solve in some test cases the three-dimensional time-dependent electromagnetic-scattering problem described in Section 2.

We consider scattering phenomena generated by the incident electromagnetic fields $\underline{\mathcal{E}}^i$, $\underline{\mathcal{B}}^i$ given by (32), (33), or by (34), (35) and we discuss the numerical results obtained both from a physical and a numerical point of view. The quantitative character of the results obtained is established. In particular, some animations relative to the numerical experiments presented can be seen on the website: *http://www.econ.unian.it/recchioni/w4/*. These animations clarify the physical meaning of the numerical experience shown. Figure 3 is taken from the animations.

Let $\underline{P} \in \mathbf{R}^3$, $\underline{\gamma} \in \partial B$ be the vectors appearing in (32), (33), or in (34), (35). In the numerical experience shown here we choose $\underline{P} = (1, 0, 0)^T$, $\underline{\gamma} = (0, 0, 1)^T$, $c = 1$ and ∂B as base point of the expansions (47), (48). We note that the value of a that defines the sphere B_a involved in the representation formula (30) is never used in the computational method and can be left undetermined. In the case of the test problems that use (32), (33) as incident electromagnetic field no numerical quadrature in the $\omega \in \mathbf{R}$ and $\underline{\alpha} \in \partial B$ variables is involved, since the incident electromagnetic field is time-harmonic and we assume that the corresponding scattered field is time harmonic with the same frequency, that is:

$$\underline{\mathcal{E}}^s(\underline{x},t)=\underline{E}_{\omega^*,\underline{\gamma}}(\underline{x})\exp(-\mathrm{i}\omega^* t),\ (\underline{x},t)\in\mathbf{R}^3\backslash\overline{\Omega}\,,\ \underline{\mathcal{B}}^s(\underline{x},t)=\underline{B}_{\omega^*,\underline{\gamma}}(\underline{x})\exp(-\mathrm{i}\omega^* t),$$

$$(\underline{x},t)\in\mathbf{R}^3\backslash\overline{\Omega}\,, \tag{61}$$

where $\underline{E}_{\omega^*,\underline{\gamma}}$, $\underline{B}_{\omega^*,\underline{\gamma}}$ are the space-dependent parts of the scattered time-harmonic electromagnetic field.

In the case of the test problems that use (34), (35) as incident electromagnetic field the integrals in (12), (13) reduce to one-dimensional integrals in the variable $\omega\in\mathbf{R}$, that is, $N_2=N_3=1$, $\underline{\alpha}_{1,1}=\underline{\gamma}$, and $w(\omega)=\zeta\exp(-\zeta^2\omega^2)$, so that we choose the quadrature rule in (26), (27) to be the Gauss-Hermite quadrature formula (see [37, p. 114]), that is, ω_i, $a_{i,1,1}$, $i=1,2,\ldots,N_1$ are the zeros of the Hermite polynomial of degree N_1 and the weights of the Gauss-Hermite quadrature formula, respectively.

Let $(\underline{x}_j,t_k)\in\mathbf{R}^3\times\mathbf{R}$, $j=1,2,\ldots,20^3$, $k=1,2,\ldots,40$ be a rectangular grid of the set $[-2,2]\times[-2,2]\times[-2,2]\times[-3,7]$ with stepsize with respect to the spatial variables (*i.e.*, the first three variables) equal to $4/20$ and with stepsize with respect to the time variable (*i.e.*, the last variable) equal to $10/40$. Since in (34), (35) the vector $\underline{P}$ is independent of the variables $\underline{x}$ and t, we choose N_1 as in [21] Section 4, that is, we consider the approximation $s^a_{\underline{\gamma}}(\underline{x},t)$ of the function $s_{\underline{\gamma}}(\underline{x},t)=\exp(-\frac{1}{4\zeta^2}[(\underline{\gamma},\underline{x})-ct]^2)$, $(\underline{x},t)\in\mathbf{R}^3\times\mathbf{R}$ given by:

$$s^a_{\underline{\gamma}}(\underline{x},t)=\sum_{j=1}^{N_1}a_{j,1,1}\exp\left(\frac{\mathrm{i}\omega_j}{c\zeta}[(\underline{x},\underline{\gamma})-ct]\right),\ (\underline{x},t)\in\mathbf{R}^3\times\mathbf{R}\,, \tag{62}$$

and we take $N_1=400$, since this guarantees that we have:

$$\frac{\left[\sum_{j=1}^{20^3}\sum_{k=1}^{40}\mid s^a_{\underline{\gamma}}(\underline{x}_j,t_k)-s_{\underline{\gamma}}(\underline{x}_j,t_k)\mid^2\right]^{1/2}}{\left[\sum_{j=1}^{20^3}\sum_{k=1}^{40}\mid s_{\underline{\gamma}}(\underline{x}_j,t_k)\mid^2\right]^{1/2}}\leq 10^{-3}\,, \tag{63}$$

when $\zeta=1$. We consider the following obstacles:

1. Sphere $r=\xi_1(\hat{\underline{x}}(\theta,\phi))=1$, $0\leq\theta\leq\pi$, $0\leq\phi<2\pi$, (see Figure 2 (1));
2. Corrugated Sphere $r=\xi_2(\hat{\underline{x}}(\theta,\phi))=1+h\ \sin^2 2\theta\ \mid\cos 2\phi\mid$, $0\leq\theta\leq\pi$, $0\leq\phi<2\pi$, (see Figure 2 (2) $h=0{\cdot}7$);
3. Cut octahedron (see Figure 2 (3));
4. Holed Sphere (see Figure 2 (4));
5. Corrugated surface:

$$r=\xi_4(\hat{\underline{x}}(\theta,\phi))=1+0{\cdot}1\left|\sum_{j=1}^{10}\frac{1}{j^3}\exp(\mathrm{i}j(\phi+\theta))\right|,\ 0\leq\theta\leq\pi,\ 0\leq\phi<2\pi. \tag{64}$$

Note that this obstacle is not represented in Figure 2. We omit the analytical expression of the surfaces of Obstacle 3, the cut octahedron and of Obstacle 4, the holed sphere, since they are

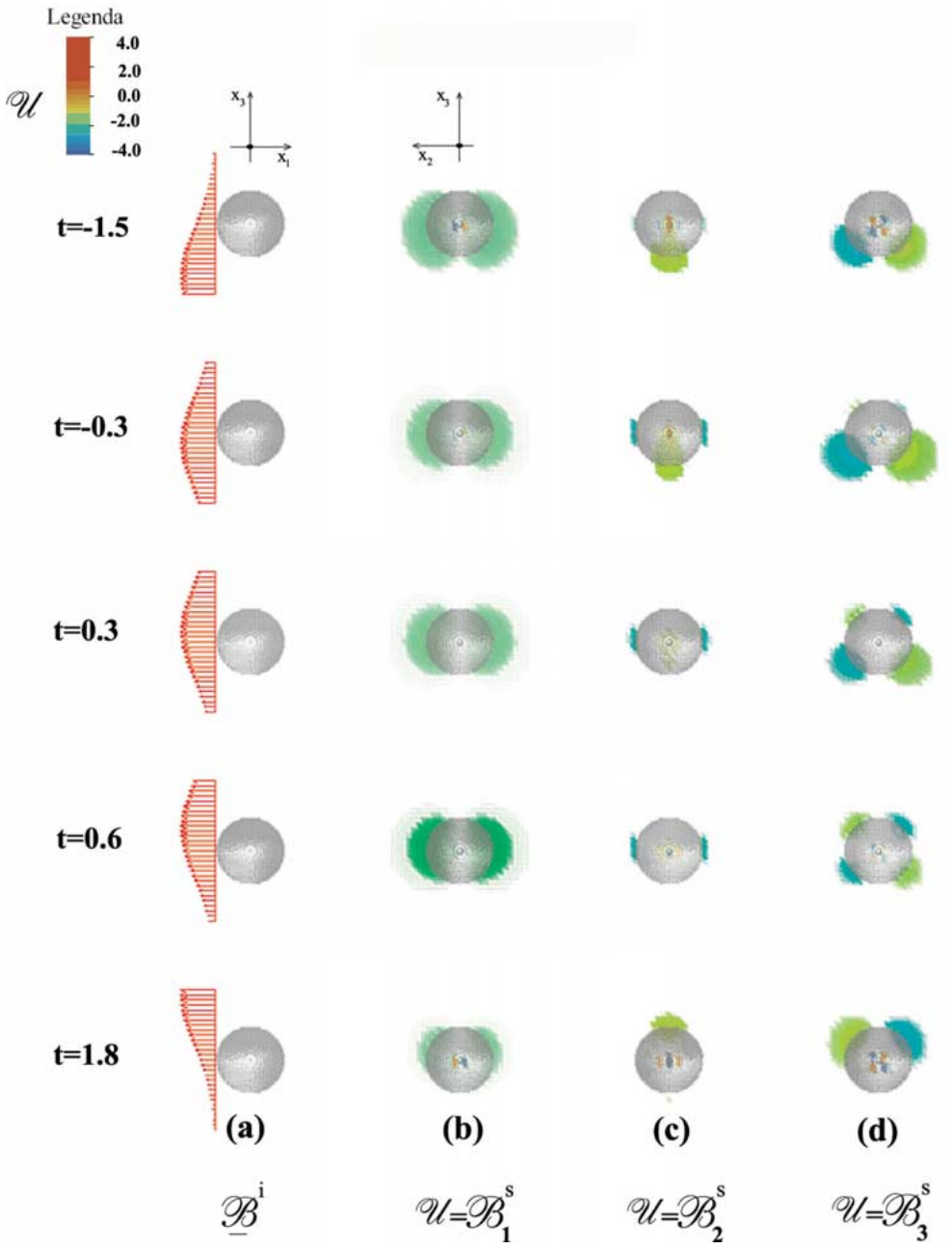

Figure 3. 'Resonance Phenomenon': the incoming magnetic induction field $\underline{\mathcal{B}}^i$ (a) ($\gamma = (0,0,1)^T$, $P = (1,0,0)^T$, $\zeta^2 = 1$) and the components of the corresponding scattered magnetic induction field $\underline{\mathcal{B}}^s$ (b), (c), (d) generated by a perfectly conducting holed sphere are shown. The arrows in column (a) represent $\underline{\mathcal{B}}^i$.

involved. We note that the origin has been chosen as the center of mass of the obstacles in the cases 1, 2, 3, 5 and that the largest sphere with center the origin contained in the cutted octahedron has radius 1. Moreover, the holed sphere is made of a sphere with center the origin and radius one with a cavity. The cavity is obtained by removing from the sphere of radius one and center the origin its intersection with a sphere with center located in the negative x_1-direction at distance from the origin $1/\cos\frac{\pi}{36}$ and radius $\tan\frac{\pi}{36}$.

The obstacles 2–5 have boundaries that are not continuously differentiable, but are only locally Lipschitz surfaces. Obstacle 1, the sphere, has a smooth boundary.

In order to choose the integer $L_{\max}$ appearing in formulae (58–60), we use the analysis shown in [19, Section 4] where it is shown that the integer $L_{\max}$ must increase when the geometry of the obstacle is of increasing complexity and we study the behavior of the approximation $\underline{F}^{S,L_{\max}}_{\omega,\underline{\gamma}}$ of $\underline{F}_{\omega,\underline{\gamma}}$ given by (60) when we choose $\underline{\alpha}=\underline{\gamma}$. This study leads us to choose $L_{\max}=16$.

Furthermore, let $\underline{F}=(F_1,F_2,F_3)^T$ be a complex vector and we define $|\underline{F}|=[\sum_{i=1}^{3}|F_i|^2]^{1/2}$; we consider a perfectly conducting sphere of radius one when $\underline{\gamma}=(0,0,1)^T$, $\underline{P}=(1,0,0)^T$. Further let $\underline{F}^{L_1}_{\omega,\underline{\gamma}}=(F^{L_1}_{1,\omega,\underline{\gamma}},F^{L_1}_{2,\omega,\underline{\gamma}},F^{L_1}_{3,\omega,\underline{\gamma}})^T$ be the truncated expansion in vector spherical harmonics of the space dependent part of the scattered electric field given in [39, p. 1882], that is $\underline{F}^{L_1}_{\omega,\underline{\gamma}}$ contains only the vector spherical harmonics with $l\leq L_1$ of the expression given in [39, p. 1182]. Note that in the case of the sphere the coefficients of the expansion are given by an explicit formula. Let $\underline{F}^{0,L_1}_{\omega,\underline{\gamma}}$ be the scattered electric field computed by the method presented in Sections 3–5 when in formula (56) we truncate the sum in l to $l\leq L_{\max}=L_1$. We consider only the zeroth order term in (56), since this is the only nonzero term of the expansion. In fact, in this case the boundary of the obstacle and the base point of the expansion are both equal to ∂B. Let L_1 be a positive integer and we define:

$$\epsilon^{L_1}_{i,\underline{F}_{\omega,\underline{\gamma}}}=\left[\frac{\sum_{j=1}^{20^3}|F^{L_1}_{i,\omega,\underline{\gamma}}(\underline{x}_j)-F^{0,L_1}_{i,\omega,\underline{\gamma}}(\underline{x}_j)|^2}{\sum_{j=1}^{20^3}|F^{L_1}_{i,\omega,\underline{\gamma}}(\underline{x}_j)|^2}\right]^{1/2},\ i=1,2,3. \tag{65}$$

We study the behavior of $\epsilon^{L_1}_{i,\underline{F}_{\omega,\underline{\gamma}}}$, $i=1,2,3$, $L_1=16$, for several values of ω, that is $\omega=1,2,4,8$ (see Table 1). Table 1 shows that the difference between $F^{L_1}_{i,\omega,\underline{\gamma}}$ and $F^{0,L_1}_{i,\omega,\underline{\gamma}}$, $i=1,2,3$, is of the order of magnitude of the error due to the quadrature rule used to compute the generalized Fourier coefficients $z_{\omega,\underline{\alpha},s,C_{\sigma,m,l}}=\int_{\partial B}(\underline{z}_{\omega,\underline{\alpha},s}(\underline{\hat{x}}),\underline{C}_{\sigma,m,l}(\underline{\hat{x}}))\mathrm{d}s(\underline{\hat{x}})$, $z_{\omega,\underline{\alpha},s,B_{\sigma,m,l}}=\int_{\partial B}(\underline{z}_{\omega,\underline{\alpha},s}(\underline{\hat{x}}),\underline{B}_{\sigma,m,l}(\underline{\hat{x}}))\mathrm{d}s(\underline{\hat{x}})$, $\sigma=0,1$, $l=1,\ldots,16$, $m=\sigma,\ldots,l$, $s=0$, of the expansion in vector spherical harmonics appearing in (56). That is, $L_1=16$ is a satisfactory choice.

Now we show some evidence of the quantitative character of the results obtained using expansion (46). We analyze the convergence of the series $\sum_{s=0}^{+\infty}z_{\omega,\underline{\gamma},s,C_{\sigma,l,m}}$, $\sum_{s=0}^{+\infty}z_{\omega,\underline{\gamma},s,B_{\sigma,l,m}}$, $\sigma=0,1$, $l=1,2,\ldots,L_{\max}$, $m=\sigma,\sigma+1,\ldots,l$, in some test cases. First we compare the analytical expression of the generalized Fourier coefficients $z^*_{\omega,\underline{\gamma},C_{\sigma,l,m}}$, $z^*_{\omega,\underline{\gamma},B_{\sigma,l,m}}$, $\sigma=0,1$, $l=1,2,\ldots,L_{\max}$, $m=\sigma,\ldots,l$ given in [39, p. 1882] with the numerically computed coefficients $\sum_{s=0}^{S}z_{\omega,\underline{\gamma},s,C_{\sigma,l,m}}$, $\sum_{s=0}^{S}z_{\omega,\underline{\gamma},s,B_{\sigma,l,m}}$, $\sigma=0,1$, $l=1,2,\ldots,L_{\max}$, $m=\sigma,\sigma+1,\ldots,l$, in the case of a time-harmonic scattering from a perfectly conducting sphere of radius R with $\omega=1$, $\underline{\gamma}=(0,0,1)^T$, $\underline{P}=(1,0,0)^T$ and $L_{\max}=16$. In Table 2 we show the behavior of the following quantity:

$$e^S_{L_{\max},R}= \tag{66}$$

$$\left[\frac{\sum_{\sigma=0}^{1}\sum_{l=1}^{L_{\max}}\sum_{m=\sigma}^{l} \mid z^{*}_{\omega,\underline{\gamma},C_{\sigma,l,m}} - \sum_{s=0}^{S} z_{\omega,\underline{\gamma},s,C_{\sigma,l,m}} \mid^2 + \mid z^{*}_{\omega,\underline{\gamma},B_{\sigma,l,m}} - \sum_{s=0}^{S} z_{\omega,\underline{\gamma},s,B_{\sigma,l,m}} \mid^2}{\sum_{\sigma=0}^{1}\sum_{l=\sigma}^{L_{\max}}\sum_{m=\sigma}^{l} \mid z^{*}_{\omega,\underline{\gamma},C_{\sigma,l,m}} \mid^2 + \mid z^{*}_{\omega,\underline{\gamma},B_{\sigma,l,m}} \mid^2}\right]^{1/2},$$

for several values of the radius R and of the parameter S. Table 2 shows that the convergence properties of the series when the distance between the obstacle $\Omega = B_R$ and the base point of the expansion $\Omega_r = B_1$ increases.

Moreover, let

$$e^{S}_{L_{\max}} = \left[\frac{\sum_{\sigma=0}^{1}\sum_{l=1}^{L_{\max}}\sum_{m=\sigma}^{l} \mid z_{\omega,\underline{\gamma},S,C_{\sigma,l,m}} \mid^2 + \mid z_{\omega,\underline{\gamma},S,B_{\sigma,l,m}} \mid^2}{\sum_{\sigma=0}^{1}\sum_{l=\sigma}^{L_{\max}}\sum_{m=\sigma}^{l} \mid \sum_{s=0}^{S} z_{\omega,\underline{\gamma},s,C_{\sigma,l,m}} \mid^2 + \mid \sum_{s=0}^{S} z_{\omega,\underline{\gamma},s,B_{\sigma,l,m}} \mid^2}\right]^{1/2}, \qquad (67)$$

in Tables 3–5 we show the behavior of $e^{S}_{L_{\max}}$ with $S = 1, 2, \ldots, 9$ and $L_{\max} = 16$ for several test cases where the incident electromagnetic field (34), (35) is the field associated to a time-harmonic linearly polarized incoming plane wave with polarization vector $\underline{P} = (1, 0, 0)^T$, and propagation direction $\underline{\gamma} = (0, 0, 1)^T$. In particular, in Table 3 and Table 4 we give $e^{S}_{L_{\max}}$ for several values of the wave number ω/c, that is, $\omega/c = 0{\cdot}5$, 1, 2, 4, 8, when the obstacle is a perfectly insulating (*i.e.*, $\chi = \infty$) cut octahedron (Table 3) or a perfectly conducting (*i.e.*, $\chi = 0$) corrugated surface (Table 4). In Table 5 we consider a corrugated sphere with electromagnetic boundary impedance $\chi = 2$ and we show $e^{S}_{L_{\max}}$ at a fixed value of the wave number $\omega/c = 10$ for different values of the height h of the corrugation. Tables 2–5 show that the convergence of the series in powers of $(\xi - 1)$, that is, the convergence of $\sum_{s=0}^{+\infty} z_{\omega,\underline{\gamma},s,C_{\sigma,l,m}}$, $\sum_{s=0}^{+\infty} z_{\omega,\underline{\gamma},s,B_{\sigma,l,m}}$, $\sigma = 0, 1$, $l = 1, 2, \ldots, L_{\max}$, $m = \sigma, \sigma + 1, \ldots, l$, depends on the magnitude of $(\omega/c) \max_{\underline{\hat{x}} \in \partial B} |\xi(\underline{\hat{x}}) - 1|$, and that, when this quantity is small enough, that is, for example in the first three rows of Table 5, the series expansion considered gives very accurate results.

We do not discuss the convergence properties of the 'Fourier integrals' (12), (13) that give $\underline{\mathcal{E}}^s$, $\underline{\mathcal{B}}^s$ or the validity of the Gauss-Hermite quadrature rule used to approximate them in our test cases, since these are standard topics in mathematical analysis.

The computational cost in terms of the number of double integrals that must be computed in order to evaluate $\underline{\mathcal{V}}^{S,N_1,1,1}_{L_{\max}}$ (see (58)), that is, the approximate series expansion of the scattered electric field $\underline{\mathcal{E}}^s$ up to order S, is given by:

$$\text{Number of Integrals} = 3N_1\, S(S+3)(L_{\max}+1)^2\,. \qquad (68)$$

We can see that the computational cost in (68) consists of a polynomial in N_1 times a polynomial in S times a polynomial in $L_{\max}$. We can use relatively large values of N_1, S and $L_{\max}$, since we make the computation of the approximations up to order S of the series in powers of $(\xi - 1)$ of the terms $\underline{E}^s_{\omega,\underline{\alpha}}$, $\omega = \omega_i$, $i = 1, 2, \ldots, N_1$, $\underline{\alpha} = \underline{\gamma}$, in parallel. Moreover, choosing $\underline{\alpha} = \underline{\gamma}$ for $\omega = \omega_i$, $i = 1, 2, \ldots, N_1$, we compute for $s_1 = 0, 1, \ldots, S$ the s_1-th order term of the expansion of $\underline{E}^s_{\omega_i,\underline{\gamma}}$ and the computation of the s_1-th order term of the expansion (56) is fully parallelizable with respect to the vector spherical harmonics involved, which means that is it is fully parallelizable with respect to $\sigma = 0, 1$, $l = 1, 2, \ldots, L_{\max}$. We note that for $s_1 = 0, 1, \ldots, S$ the computation of the (s_1+1)-th-order term in the perturbation series involves the knowledge of the s_1-th-order term. Finally, the summation that defines the quadrature rule can be computed in parallel. Thus, several different parallel architectures can be used profitably to reduce the time needed to compute the approximations $\underline{\mathcal{V}}^{S,N_1,1,1}_{L_{\max}}$ and

Table 6. Time versus number of processors

processors	seconds
3	858·73
6	429·59
12	215·04
24	107·80
30	86·38
60	43·30
120	21·51

$\underline{\mathcal{U}}_{L_{\max}}^{S,N_1,1,1}$ in (58) and (59) of the solution $\underline{\mathcal{E}}^s$, $\underline{\mathcal{B}}^s$ of problem (1–5), (7), (8). Formulae similar to (68) can be derived to express the computational cost of the method described in Sections 3–5 in the general case when $N_2 \neq 1$, $N_3 \neq 1$.

The algorithm previously described has been coded in Fortran 90 language and tested on a cluster of four Alpha Digital workstations each one having four processors and on a Cray T3E machine with 256 processors in 'Multiple Instructions Multiple Data' programming mode using MPI as 'message passing' library.

Table 6 shows the execution time required versus the number of processors used by the algorithm on the Cray T3E machine to compute $\sum_{s=0}^{4} z_{\omega_i,\underline{\gamma},s,C_{\sigma,l,m}}$, and $\sum_{s=0}^{4} z_{\omega_i,\underline{\gamma},s,B_{\sigma,l,m}}$, $i = 1, 2, \ldots, N_1$, $\sigma = 0, 1$, $l = 1, 2, \ldots, L_{\max}$, $m = \sigma, \ldots, l$, $N_1 = 400$, $L_{\max} = 16$, relative to a perfectly conducting holed sphere, that is $\chi = 0$, and an incident electromagnetic field given by (34), (35) with $\underline{\gamma} = (0, 0, 1)^T$, $\underline{P} = (1, 0, 0)^T$, $\zeta = 1$ (see Figure 3). The time is measured using the (Fortran) routine $rtc()$ of the Cray T3E machine that gives the real-time clock in clicks where a click corresponds to 3·333e-09 seconds. Table 6 shows that the parallel performance of our algorithm on a parallel computer is really excellent in fact when passing from 3 to 120 processors, that is, by multiplying the number of processors by 40, we divide the corresponding execution time by 858·73/21·51≈39·92 so that we have a speed-up factor of approximately 39·92/40=0·998.

We comment on some numerical results that are interesting from a physical point of view obtained in one of the experiments described above.

Let

$$Z_{20} = \{ (x, y, z)^T \in \mathbf{R}^3,\ x = -2 + \frac{4}{20} i,\ y = -2 + \frac{4}{20} j, z = -2 + \frac{4}{20} k,\ i, j, k = 0, 1, \ldots,\ 20\}. \tag{69}$$

In Figure 3 (a) we show the incident magnetic-induction vector $\underline{\mathcal{B}}^i(\underline{x}, t)$ for five values of the time variable t, $t = -1{\cdot}5, -0{\cdot}3, 0{\cdot}3, 0{\cdot}6, 1{\cdot}8$, when $\underline{x}$ belongs to a plane parallel to the plane containing the origin and whose normal direction is given by $[\underline{\gamma}, \underline{P}] = (0, 1, 0)^T$ and located on top of the hole. In Figures 3 (b), (c), (d) we show a color map of the first component of $\underline{\mathcal{B}}^s$ (column (b)), of the second component of $\underline{\mathcal{B}}^s$ (column (c)) and of the third component of $\underline{\mathcal{B}}^s$ (column (d)), respectively, when $\underline{x} \in Z_{20}$ and $t = -1{\cdot}5, -0{\cdot}3, 0{\cdot}3, 0{\cdot}6, 1{\cdot}8$. We choose the time variable t such that the maximum norm of the incident magnetic-induction vector field is located, first at the bottom of the obstacle, then in the middle of the obstacle and finally at the top of Obstacle 4, the holed sphere.

Note that the point of view of Figure 3 (a) is different from the point of view of Figures 3 (b), (c), (d) (see the frames of reference shown on the top column (a) and (b) of Figure 3). In fact, in Figure 3 (a) we look on the side of the hole and in Figures 3 (b), (c), (d) we look in front of the hole.

We can see that the energy is trapped (the first and the second rows of Figures 3 (b), (c), (d)), then irradiated (the third and the fourth rows of Figures 3 (b), (c), (d)), then trapped (the last row of Figures 3 (b), (c), (d)) by the hole when the incident field goes through the obstacle. This means that some kind of 'resonance' phenomenon takes place. This 'resonance' phenomenon is similar that observed in [19, Figures 6, 7] and in acoustics in [21, Figure 5].

Some animations relative to the experiments discussed previously can be found on the website: *http://www.econ.unian.it/recchioni/w4/* .

7. Conclusions

In this paper a method to solve time-dependent Maxwell equations in an isotropic homogeneous medium has been introduced. This method fulfills conditions $(r1)$–$(r4)$ of the Introduction. In fact, the approximations of the electric and magnetic fields considered are divergence-free by construction. Moreover, the computation of these approximations in the particular implementation of the method presented in this paper involves only the solution of 'diagonal' linear systems of equations. Finally, the method is highly parallelizable (see Table 6), since we can compute simultaneously the time-harmonic fields appearing in formulas (26), (27) and the computation of each time-harmonic field with the operator-expansion method is highly parallelizable. The limit of the implementation proposed here is that it does not fulfill completely condition $(r5)$. In fact, it is efficient and accurate when obstacles whose shape is 'near' to the shape of a sphere are considered. However, as noted previously non-trivial obstacles are 'near' the sphere in this context; see for example the cut octahedron (see Table 3) and the corrugated surface (see Table 4). Finally, we note that the computational cost of the proposed method is limited. In fact, it is linear in the number N_1 of the time frequencies involved, it is quadratic in the parameter S related to the expansion and in the number of coefficients $2(L_{\max}+2)L_{\max}$ of the vector spherical harmonics involved. Moreover, since the computation of the N_1 time-harmonic scattered fields can be carried out in parallel and also the $2(L_{\max}+2)L_{\max}$ coefficients of the expansion in vector spherical harmonics at each order in the operator expansion can be computed in parallel, the method can be considered an efficient tool to solve time-dependent Maxwell equations when parallel computing is available. The version of the operator expansion method presented in this paper is limited to obstacles 'near' the sphere and is very powerful (*i.e.*, satisfies $(r1)$–$(r4)$, is highly parallelizable, its computational complexity is competitive with the complexity of other existing methods). At the price of reducing the performance obtained, the operator-expansion method can be adapted for arbitrary obstacles. Further investigation will needed to study implementations of the method capable to solve transmission and scattering problems in the presence of dispersive materials. Note that the method presented here can be used with slight modifications to solve transmission problems when the electric permittivity ϵ and the magnetic permeability μ are piecewise constant functions of the spatial variables. Finally, we plan to develop a new version of the operator-expansion method that removes the assumption of the existence of a coordinate system (η_1, η_2, η_3) such that the boundary of the obstacle $\partial\Omega$ admits a global representation in this coordinate system, *i.e.*, it can be represented as a function of one coordinate variable

in terms of the other two coordinate variables. It is easy to see that it is possible to weaken this hypothesis, assuming only the existence of a local representation of $\partial\Omega$. Thus, $\partial\Omega$ can be obtained by matching local representations with respect to several different coordinate systems. This new version of the method could solve efficiently scattering problems from obstacles whose shapes can be considered arbitrary for all practical purposes.

Acknowledgments

The numerical experiments shown in this paper have been made possible by the support and sponsorship of CINECA (Consorzio Interuniversitario Nord Est Calcolo Automatico) - Casalecchio di Reno (Bologna) - Italy through a grant account on the T3E computer facility.

References

1. C.D. Munz and P. Ommes, A three-dimensional finite-volume solver for the Maxwell equations with divergence cleaning on unstructured meshes. *Comp. Phys. Comm.* 130 (2000) 83–117.
2. F. Assous, P. Degond, E. Heintze, P. Raviart and J. Segrè, On a finite-element method for solving the three-dimensional Maxwell equations. *J. Comp. Phys.* 109 (1993) 222–237.
3. A. Taflove and S.C. Hagness, *Computational Electrodynamics: The Finite-Difference Time Domain Method* 2nd Edition. Boston: Artech House (2000) 878 pp.
4. J.F. Lee, R. Lee and A. Cangellaris, Time-domain finite elements methods. *IEEE Trans. Antennas Propag.* 45 (1997) 430–442.
5. N.K. Madsen and R.W. Ziolkowski, A three-dimensional modified finite volume technique for Maxwell's equations. *Electromagnetics* 10 (1990) 147–161.
6. F. Edelvik and G. Ledfelt, Explicit hybrid time domain solver for the Maxwell equations in 3D. *J. Scient. Comp.* 15 (2000) 61–78.
7. J.M. Song and W.C. Chew, Multilevel fast-multipole algorithm for solving combined field integral equations of electromagnetic scattering. *Microwave Opt. Tech. Lett.* 10 (1995) 14–19.
8. A.A. Ergin, B. Shanker and E. Michielssen, Fast evaluation of three-dimensional transient wave field using diagonal translation operators. *J. Comp. Phys.* 146 (1998) 157–180.
9. K.S. Yee, Numerical solution of initial boundary value problems involving Maxwell's equations in isotropic media. *IEEE Trans. Antennas Propagation* 14 (1966) 302–307.
10. F.L. Teixeira and W.C. Chew, Lattice electromagnetic theory from a topological viewpoint. *J. Math. Phys.* 40 (1999) 169–187.
11. C.D. Munz, R. Schneider, E. Sonnendrücker and U. Voss, Maxwell's equations when the charge conservation is not satisfied. *Compt. Rendus Académie des Sci. Paris* 328 (1999) 431–436.
12. K.L. Shlager, J.G. Maloney, S.L. Ray and A.F. Peterson, Relative accuracy of several finite-difference time-domain methods in two and three dimensions. *IEEE Trans. Antennas Propagation* 41 (1993) 1732–1737.
13. G. Mur, Absorbing boundary conditions for the finite-difference approximation of the time-domain electromagnetic-field equations. *IEEE Trans. Electromagn. Compatibility* 23 (1982) 377–382.
14. Y. Lu and C.Y. Shen, A domain decomposition finite-difference method for parallel numerical implementation of time-dependent Maxwell's equations. *IEEE Trans. Antennas Propagation* 45 (1997) 556–562.
15. F. Assous, P. Degond and J. Segrè, Numerical approximation of the Maxwell equations in inhomogeneous media by a P^1 conforming finite element method. *J. Comp. Phys.* 126 (1996) 363–380.
16. B. Jiang, J. Wu and L.A. Povinelli, The origin of spurious solutions in computational electromagnetics. *J. Comp. Phys.* 125 (1996) 104–123.
17. G. Manara, A. Monorchio and R. Reggiannini, A space-time discretization criterion for a stable time-marching solution of the electric field integral equation. *IEEE Trans. Antennas Propagation* 45 (1997) 527–532.
18. R. Coifman, V. Rokhlin and S. Wandzura, The fast multipole method for wave equation: a pedestrian prescription. *IEEE Antennas Propag. Mag.* 35 (1993) 7–12.
19. L. Fatone, C. Pignotti, M.C. Recchioni and F. Zirilli, Time harmonic electromagnetic scattering from a bounded obstacle: An existence theorem and a computational method. *J. Math. Phys.* 40 (1999) 4859–4887.

20. E. Heyman, Time-dependent plane-wave spectrum representations for radiation from volume source distributions. *J. Math. Phys.* 37 (1996) 658–681.
21. E. Mecocci, L. Misici, M.C. Recchioni and F. Zirilli, A new formalism for time dependent wave scattering from a bounded obstacle. *J. Acoust. Soc. Amer.* 107 (2000) 1825–1840.
22. D.M. Milder, An improved formalism for wave scattering from rough surface. *J. Acoust. Soc. Amer.* 89 (1991) 529–541.
23. D.M. Milder, Role of the admittance operator in rough-surface scattering. *J. Acoust. Soc. Amer.* 100 (1996) 759–768.
24. D.M. Milder, An improved formulation of coherent forward scatterer from random rough surfaces. *Waves Rand. Med.* 8 (1998) 67–78.
25. L. Misici, G. Pacelli and F. Zirilli, A new formalism for wave scattering from a bounded obstacle. *J. Acoust. Soc. Amer.* 103 (1998) 106–113.
26. F. Mariani, M.C. Recchioni and F. Zirilli, The use of the Pontryagin maximum principle in a furtivity problem in time dependent acoustic obstacle scattering. *Waves Rand. Med.* 11 (2001) 549–575.
27. F. Mariani, M.C. Recchioni and F. Zirilli, A perturbative approach to acoustic scattering from a vibrating bounded obstacle. *J. Comp. Acoust.* 10 (2002) 349–384.
28. M.C. Recchioni and F. Zirilli, The use of wavelets in the operator expansion method for time dependent acoustic obstacle scattering. Submitted to *Siam J. Scient. Comp.*
29. D.M. Milder, An improved formalism for electromagnetic scattering from a perfectly conducting rough surface. *Radio Sci.* 31 (1996) 1369–1376.
30. S. Piccolo, M.C. Recchioni and F. Zirilli, The time harmonic electromagnetic field in a disturbed half-space: An existence theorem and a computational method. *J. Math. Phys.* 37 (1996) 2762–2786.
31. R.A. Smith, The operator expansion formalism for electromagnetic scattering from rough dielectric surfaces. *Radio Sci.* 31 (1996) 1377–1385.
32. R. Coifman, A. McIntosh and Y. Meyer, L'intégrale de Cauchy définit un opérateur borné sur L^2 pour les courbes lipschitziennes. *Annals Math.* 116 (1982) 361–387.
33. G. Verchota, Layer potentials and boundary value problems for Laplace's equation in Lipschitz domains. *J. Funct. Anal.* 59 (1984) 572–611.
34. J. Nečas, *Les Méthodes Directes en Théorie des Équations Elliptiques*. Paris: Masson & Cie. Publ. (1967) 351 pp.
35. J.A. Stratton, *Electromagnetic Theory*. New York: McGraw-Hill Book Company (1941) 615 pp.
36. T.S. Angell and A. Kirsch, The conductive boundary condition for Maxwell's equations. *SIAM J. Appl. Math.* 52 (1992) 1597–1610.
37. A. Ghizzetti and A. Ossicini, *Quadrature Formulae*. Basel: Birkhäuser Verlag (1970) 191 pp.
38. M. Abramowitz and I.A. Stegun, *Handbook of Mathematical Functions*. New York: Dover (1970) 1046 pp.
39. P.M.Morse and H.Feshbach, *Methods of Theoretical Physics Vol II*. New York: Mc Graw Hill (1953) 1978 pp.